TARDEC

---TECHNICAL REPORT---

THE NATION'S LABORATORY FOR ADVANCED AUTOMOTIVE TECHNOLOGY

WINNER OF THE 1994 FEDERAL QUALITY IMPROVEMENT PROTOTYPE AWARD

No._____

Damage Behavior of Composite Structures and Joints at Room and Elevated Temperatures

Final Report: Phase I

Contract No: DAAE07-96-C-X-121

March 1998

Feridun Delale
Ardie D. Walser
By Benjamin M. Liaw

Approved For Public Release:
Distribution is Unlimited

U.S. Army Tank-Automotive Research,
Development, and Engineering Center
Detroit Arsenal
Warren, Michigan 48397-5000

REPORT DOCUMENTATION PAGE

Form Approved
OMB No. 0704-0188

1a. REPORT SECURITY CLASSIFICATION: Unclassified	1b. RESTRICTIVE MARKINGS
2a. SECURITY CLASSIFICATION AUTHORITY	3. DISTRIBUTION / AVAILABILITY OF REPORT
2b. DECLASSIFICATION / DOWNGRADING SCHEDULE	
4. PERFORMING ORGANIZATION REPORT NUMBER(S)	5. MONITORING ORGANIZATION REPORT NUMBER(S)
6a. NAME OF PERFORMING ORGANIZATION: The Research Foundation of CUNY on behalf of The City College of CUNY; 6b. OFFICE SYMBOL (If applicable)	7a. NAME OF MONITORING ORGANIZATION: U.S. Army (TARDEC)
6c. ADDRESS (City, State, and ZIP Code)	7b. ADDRESS (City, State, and ZIP Code)
8a. NAME OF FUNDING / SPONSORING ORGANIZATION: U.S. Army (TARDEC); 8b. OFFICE SYMBOL (If applicable)	9. PROCUREMENT INSTRUMENT IDENTIFICATION NUMBER
8c. ADDRESS (City, State, and ZIP Code): U.S. Army Tank-Automotive Commander, Warren, MI. 48397-5000	10. SOURCE OF FUNDING NUMBERS: PROGRAM ELEMENT NO. / PROJECT NO. / TASK NO. / WORK UNIT ACCESSION NO.

11. TITLE (Include Security Classification)

Damage Behavior of Composite Structures and Joints at Room and Elevated Temperatures

12. PERSONAL AUTHOR(S)

Feridun Delale, Ardie D. Walser, Benjamin M. Liaw

13a. TYPE OF REPORT	13b. TIME COVERED	14. DATE OF REPORT (Year, Month, Day)	15. PAGE COUNT
Final	FROM 96 MAY TO 97OCT	1998, March 31	58

16. SUPPLEMENTARY NOTATION

17. COSATI CODES			18. SUBJECT TERMS (Continue on reverse if necessary and identify by block number)
FIELD	GROUP	SUB-GROUP	Composite Materials, SEM testing, MTS testing, Laser Interferometry, stress-strain curves, FEM modeling, fiber, matrix, interface

19. ABSTRACT (Continue on reverse if necessary and identify by block number)

In this project the damage behavior of S2 glass/ toughened epoxy composites of various lay-up configurations was studied under tensile and bending loads at room and elevated temperatures. First miniature dog-bone shaped specimens were tested in situ in a scanning electron microscope (SEM) at room temperature and also at 75^0 C and 125^0 C under tensile loading. For each specimen, using the load and displacement data a stress-strain curve was constructed. It was observed that the curve, which is linear in the beginning, becomes non-linear at higher loads due to damage in the specimen. This damage consisted mainly of debonding along the fiber/matrix interface and fiber breaking and was recorded through microphotographs.

Continue...→

20. DISTRIBUTION / AVAILABILITY OF ABSTRACT	21. ABSTRACT SECURITY CLASSIFICATION	
☐ UNCLASSIFIED/UNLIMITED ☒ SAME AS RPT. ☐ DTIC USERS		
22a. NAME OF RESPONSIBLE INDIVIDUAL	22b. TELEPHONE (Include Area Code)	22c. OFFICE SYMBOL

DD Form 1473, JUN 86 *Previous editions are obsolete.* SECURITY CLASSIFICATION OF THIS PAGE

Block Number: 19

Next, standard-size specimens of the same material were tested in a universal testing machine (MTS) under tensile loads and again from room temperature to 125^0 C. The specimens had four different lay-up configurations. Again, for each specimen a stress-strain curve was constructed. The results indicate that the lay-up configuration and temperature have significant effect on the ultimate strength, stiffness and failure strain of the composite.

During the next phase of the project the same composite was also tested under 3-point bending loads again at room and elevated temperatures. Mid-span stress versus normalized displacement curves were constructed for each test. The results show that temperature and lay-up architecture affect significantly the stiffness, deformation and ultimate strength of the composite under bending loads.

One of the objectives of the project was to measure strains at high temperature using the laser interferometry technique. During this period the experimental set-up was perfected and the technique was successfully tested on aluminum specimens subjected to bending loads. The tests on composite specimens will be carried out during the second phase of the project.

Finally, a finite element model based on micromechanics was developed. The damage observed during testing, that is to say, fiber breaking and interfacial debonding was incorporated into the model. The numerical calculations indicate that the observed behavior can be simulated extremely well with the proper choice of interface frictional stress.

ACKNOWLEDGEMENTS

The authors would like to acknowledge the financial support provided by TARDEC in carrying out this study. Mr. Gregory Chappelle worked tirelessly as liaison to make this project a success. Dr. B.B. Raju as monitor provided valuable comments and guidance, which are sincerely appreciated. The efforts of the previous monitors Ms. Rhonda Dunfee and Mr. Scott Hodges are also gratefully acknowledged. Several graduate and undergraduate students at CCNY participated in this project: Dr. Hanqing Zhang; Mr. Thomas Cheung; Mr. Xiang Long; Mr. Brian Cooblall; Ms. Blanca Marmolejo; Mr. William Rodriguez; Mr. Denzil John. Their efforts are appreciated.

TABLE OF CONTENTS

SECTION		PAGE
1.0	**INTRODUCTION**	9
2.0	**OBJECTIVE**	9
3.0	**CONCLUSIONS**	10
4.0	**RECOMMENDATIONS**	10
5.0	**DISCUSSION**	11
6.0	**TASKS IN PHASE I**	11
6.1	*THE MATERIAL AND SPECIMENS*	11
6.2	*TENSILE TESTING IN SEM*	12
	6.2.1 Description of Experiments	12
	6.2.2 Results	12
	6.2.3 Discussion and Conclusions	13
6.3	*TESTING IN MTS*	13
	6.3.1 Description of Experiments	13
	6.3.2 Results	13
	6.3.3 Short Specimen Testing	14
	6.3.4 Discussion and Conclusions	14
	6.3.5 Comparison of SEM and MTS Results	15
6.4	*THE THREE-POINT BENDING TESTS IN MTS*	15
	6.4.1 Description of Experiments	15
	6.4.2 Results	15
	6.4.3 Discussion and Conclusions	16
6.5	*INTERFEROMETRIC STRAIN DISPLACEMENT GAUGE*	16
	6.5.1 Experiments	16
	6.5.1.1 Interference Fringe Pattern	17
	6.5.1.2 Strain Measurement	17
	6.5.1.3 Experimental Technique	17
	6.5.2 Results	18
	6.5.2.1 Three Point Bending	18
	6.5.3 Conclusions	18
6.6	*THE MICOSTRUCTURAL MODEL AND THE FINITE ELEMENT RESULTS*	18
	6.6.1 Description of the Model	18
	6.6.2 Results and Discussion	19
	6.6.3 Conclusions	19

PAGE

7 **REFERENCES** 19

APPENDIX A: Description of Phase II of Project A1
APPENDIX B: Abstracts Submitted for Presentation B1

LIST OF FIGURES

		PAGE
Figure 1	Specimen used in SEM testing	21
Figure 2	Specimen used in MTS testing	21
Figure 3	Specimen used in MTS 3-point bending tests	22
Figure 4	Specimen used in SEM testing	23
Figure 5	Comparison of strength for various lay-up configurations under tensile load at room temperature	23
Figure 6	Microphotographs showing fiber breakage and interfacial debonding	24
Figure 7	Composites failure at $\pm 45^0$ (at 80 MPa)	25
Figure 8	Comparison of room temperature and 125^0C results for $[0^0]_{8\text{-ply}}$ specimens	26
Figure 9	Comparison of room temperature and 125^0C results for $[+45^0/-45^0/+45^0/-45^0]_s$ specimens.	26
Figure 10	Comparison of MTS tensile results for various lay-up configurations at room temperature (Long specimens)	27
Figure 11	Comparison of tensile stress-strain curves at 75^0C for various lay-up configurations (Long specimens)	27
Figure 12	Comparison of tensile stress-strain curves at 125^0C for various lay-up configurations (Long specimens)	28
Figure 13	Effect of temperature on $[0^0]_{24\text{-ply, Type 2}}$ specimens	28
Figure 14	Effect of temperature on $[0^0/0^0/90^0/90^0/0^0/0^0/90^0/90^0/0^0/0^0/90^0/90^0]_s$ specimens	29
Figure 15	Effect of temperature on $[0^0{}_3/+45^0{}_3/90^0{}_3/-45^0{}_3]_s$ specimens	29
Figure 16	Effect of temperature on $[+45^0{}_3/-45^0{}_3]_{2s}$ specimens	30
Figure 17	Effect of lay-up configuration at room temperature (Short specimens)	30
Figure 18	Effect of lay-up configuration at 75^0C (Short specimens)	31
Figure 19	Effect of lay-up configuration at 125^0C (Short specimens)	31
Figure 20	Effect of temperature on $[0^0/0^0/90^0/90^0/0^0/0^0/90^0/90^0]_s$ (Short specimens)	32
Figure 21	Effect of temperature on $[0^0/0^0/+45^0/+45^0/90^0/90^0/-45^0/-45^0]_s$ (Short specimens)	32
Figure 22	Effect of temperature on $[+45^0/+45^0/-45^0/-45^0/+45^0/+45^0/-45^0/-45^0]_s$ (Short specimens)	33
Figure 23	Three-Point Bending Test Set-Up	33
Figure 24	Effect of lay-up at room temperature (3-point bending)	34
Figure 25	Effect of lay-up at 75^0C temperature (3-point bending)	34
Figure 26	Effect of lay-up at 125^0C temperature (3-point bending)	35
Figure 27	Effect of Temperature for $[0^0]_{24\text{-ply, type2}}$ (Three Point Bending)	35
Figure 28	Effect of Temperature for $[0^0{}_3/90^0{}_3]_{2s, \text{type2}}$ (Three Point Bending)	36

PAGE

Figure 29 Effect of Temperature for $[0^0_3/+45^0_3/90^0_3/-45^0_3]_{s,\ type2}$ (Three Point Bending) 36
Figure 30 Effect of Temperature for $[+45^0_3/-45^0_3]_{2s,\ type2}$ (Three Point Bending) 37
Figure 31 Schematic of interferometric strain displacement gauge (ISDG) setup 37
Figure 32 Photograph of the actual IDSG set-up used for the three-point bending measurements. 38
Figure 33 A photograph of two indentations in S2-Glass/Toughened Epoxy Composites enlarged 200 times. 38
Figure 34 The Interference pattern from two indentations in an aluminum sample. 39
Figure 35 The variation of the photodetector signal as the interference pattern moves across the slit as the sample is loaded. Each of the first two dips represents a dark fringe. 40
Figure 36 Comparison of the standard MTS results with that of the IDSG for 3 Point Bending measurements on an aluminum sample. 40
Figure 37 Three-Fiber Model of Unidirectional Lamina Damaged by Fiber Break 41
Figure 38 The finite element mesh 42
Figure 39 Comparison between simulated FE and experimental stress-strain curves for S2 glass toughened epoxy $[0^0]_{8\text{-ply}}$ 43

LIST OF TABLES

		PAGE
Table 1.	Lay-up configurations for specimens used in MTS tensile testing	44
Table 2.	Lay-up configurations for specimens used in MTS 3-point bending testing	45
Table 3.	Comparison of theoretical and experimental values of stiffness for various lay-up configurations	46
Table 4.	Variation of stiffness and strength of the composite with various lay-up configurations	46

ABSTRACT

In this project the damage behavior of S2 glass/ toughened epoxy composites of various lay-up configurations was studied under tensile and bending loads at room and elevated temperatures. First miniature dog-bone shaped specimens were tested in situ in a scanning electron microscope (SEM) at room temperature and also at 75^0 C and 125^0 C under tensile loading. For each specimen, using the load and displacement data a stress-strain curve was constructed. It was observed that the curve, which is linear in the beginning, becomes non-linear at higher loads due to damage in the specimen. This damage consisted mainly of debonding along the fiber/matrix interface and fiber breaking and was recorded through microphotographs.

Next, standard-size specimens of the same material were tested in a universal testing machine (MTS) under tensile loads and again from room temperature to 125^0 C. The specimens had four different lay-up configurations. Again, for each specimen a stress-strain curve was constructed. The results indicate that the lay-up configuration and temperature have significant effect on the ultimate strength, stiffness and failure strain of the composite.

During the next phase of the project the same composite was also tested under 3-point bending loads again at room and elevated temperatures. Mid-span stress versus normalized displacement curves were constructed for each test. The results show that temperature and lay-up architecture affect significantly the stiffness, deformation and ultimate strength of the composite under bending loads.

One of the objectives of the project was to measure strains at high temperature using the laser interferometry technique. During this period the experimental set-up was perfected and the technique was successfully tested on aluminum specimens subjected to bending loads. The tests on composite specimens will be carried out during the second phase of the project.

Finally, a finite element model based on micromechanics was developed. The damage observed during testing, that is to say, fiber breaking and interfacial debonding was incorporated into the model. The numerical calculations indicate that the observed behavior can be simulated extremely well with the proper choice of interface frictional stress.

1.0 INTRODUCTION

In this study S2 glass/toughened epoxy composite specimens of various configurations were tested in room and at elevated temperatures under tensile and 3-point bending loads. The goal was to ascertain the damage behavior of the composite under various loading conditions and to determine the effect of temperature and lay-up configurations on the stiffness, ultimate strength, and failure modes of the material. A finite element model based on micromechanics and the damage observed was to be developed to explain and simulate the observed behavior. To achieve these goals an extensive testing program combined with finite element modeling was undertaken.

First miniature composite specimens were tested in situ in a Scanning Electron Microscope (SEM) at room and elevated temperatures. The load and displacement for each specimen were recorded until failure. At various stages of the loading sequence microphotographs were taken to document to progression of damage. The tests were carried out at room and elevated temperatures.

Next, standard-size composite specimens were subjected to tensile loads in a Universal Testing Machine (MTS), first at room temperature, and later at 75^0C and 125^0C. The results were checked for consistency with those obtained in SEM. Also composite coupons were tested under 3-point bending again at room and 75^0C and 125^0C.

One of the challenges of this project has been to develop a laser interferometry technique to measure the strains under tension and bending, especially at higher temperatures. Much effort was expanded to make the technique work. We are pleased to report that satisfactory strain results were obtained for a specimen under 3-point bending and the feasibility of the technique has been demonstrated. Now the actual tests can be carried out during the option phase of this project. Also an analytical model was developed to simulate and explain the observed behavior of the composite. The model is based on micromechanics and incorporates elements of damage observed during testing. The calculations were done using the finite element program ABAQUS. As will be seen later, the match between numerical results and test data was quite good.

As can be deduced from this overview, by and large the objectives of the project were completed. Below, we give a detailed accounting of the techniques used, the results obtained, followed by a discussion of these results.

2.0 OBJECTIVES:

Overall objective of the Program:

Investigate the damage behavior of S2glass/toughened epoxy composites at room and elevated temperatures subjected to tensile and bending loads.

Application Area:

Automotive structures, Army vehicle structures and armors, such as CAV/ATD.

Detailed Objectives:

- Testing of S2glass/toughened epoxy composite specimens in Scanning Electron Microscope (SEM) under tensile loading at room and elevated temperatures.

- Testing of same composite specimens in a Universal Testing Machine (MTS) under tensile and bending loads at room and elevated temperatures.

- Strain measurements in same composite specimens using laser interferometry, also at room and elevated temperatures.

- Develop a Finite Element model based on micromechanics to simulate or predict observed damage behavior.

3.0 CONCLUSIONS

In this study S2glass/toughened epoxy composite specimens were tested in SEM and MTS to assess their damage behavior under tensile and bending loads. The effect of temperature was also investigated. The behavior of the composite was assessed through the stress-strain curves obtained during testing. Also a Finite Element model based on micromechanics to simulate the observed damage behavior was developed. Based on the testing and analysis carried out for this contract, the following conclusions can be listed:

- The stress-strain curves are linear at low load level and become non-linear when loads are increased and damage in the composite accumulates.

- Under tensile loading the lay-up configuration greatly affects the strength and stiffness of the composite.

- Under tensile loading, the strength and stiffness of the composite decreases with increasing temperature.

- Under bending loads, again the strength and stiffness of the composite are significantly affected by varying the lay-up configuration.

- Under bending loads, for the same lay-up, the strength and stiffness of the composite decrease with increasing temperature.

- The local strains in the composite can be also measured using the laser interferometry technique.

- The Finite Element model developed for this study can simulate quite well the stress-strain curve obtained experimentally.

4.0 RECOMMENDATIONS:

Based on the results obtained so far, the following additional experimental and analytical work appears to be the logical follow-up, which constitutes Phase II of this project:

- In SEM, conclude higher temperature experiments for the remaining lay-up configurations.

- Apply the laser interferometry technique to composite specimens.

- Extend MTS testing to include composite joints

- Develop a Finite Element model to simulate damage in composite joints. The write-up describing this phase of the project is given in Appendix A.

5.0 DISCUSSION

Composite materials are finding wider areas of applications due to their very high strength-to-weight and stiffness-to-weight ratios. Applications in automotive industry and Army vehicles are becoming widespread. For example the Army's CAV/ATD (Composite Armored Vehicle / Advanced Technology Demonstrator) was developed using S2glass/toughened epoxy composites in its structure and armor. Thus, it is clear that a thorough understanding of the damage behavior of the material under various loading conditions and high and low temperatures is necessary to be able to design with these new materials. This study was designed to understand the mechanical behavior of S2glass/toughened epoxy composites.

For this purpose the composite was tested under tensile and bending loads at room and elevated temperatures up to 125^{0}C. The strength, stiffness and failure of strain were assessed for various lay-up configurations and as indicated before at room and elevated temperatures. Also a finite element model based on micromechanics was developed to simulate the observed behavior.

6.0 TASKS IN PHASE I

6.1 THE MATERIAL AND SPECIMENS

As mentioned earlier the material used in this project is S2 glass/toughened epoxy composite. The fibers are S2 glass (round glass: 750ya/lb.) procured from Corning Glass and the matrix is a toughened epoxy resin (NCT-301) procured from Newport Adhesives and Composites, Inc. The composite was manufactured by Composiflex, Inc., with the specified fiber volume fraction of 55%.
For SEM specimens, 2.5" X 4" (Fibers along 2.5" direction) 8-ply and 16-ply flat composite panels were manufactured with the following lay-up configurations:

$[0^0]_8$;

$[0^0/90^0/0^0/90^0]_s$;

$[0^0/+45^0/90^0/-45^0]_s$;

$[+45^0/-45^0/+45^0/-45^0]_s$;

$[0^0]_{16}$;

$[0^0/0^0/90^0/90^0/0^0/0^0/90^0/90^0]_s$;

$[0^0/0^0/45^0/45^0/90^0/90^0/-45^0/-45^0]_s$;

$[45^0/45^0/-45^0/-45^0/45^0/45^0/-45^0/-45^0]_s$.

The miniature dog-bone shaped specimens for SEM were machined at CCNY's Material Processing Laboratory. For this purpose, the panels were cut into strips and then machined into dog-bone shape using a diamond wheel cutter and a hand held grinder. The surfaces of the specimen were polished for SEM observations. The dimensions of a typical SEM specimen are shown in Fig.1. For the MTS tensile testing, the same composite material (S2 glass/toughened epoxy) was used. The specimens were two type of dog-bone shaped specimens, with dimensions as shown in Fig.2. The lay-up configurations are listed in Table1.

For 3-point bending MTS tests, rectangular shaped coupons were used. The dimensions of the coupons and the various lay-up configurations are given in Fig.3 and Table 2 respectively.

6.2 TENSILE TESTING IN SEM

As stated earlier dog-bone shaped miniature composite specimens were tested in situ in SEM, first at room and later at elevated temperatures. The purpose was to observe and record the damage in the composite from start to failure and correlate it with the applied load.

6.2.1 Description of Experiments

The composite specimens were mounted onto a loading/heating substage and put in the chamber of SEM. The experimental set-up is shown in Fig. 4. The load was increased until failure, and the corresponding displacements were recorded. The progression of damage was monitored on the screen of the SEM, and when warranted the loading was stopped and microphotographs were taken. The load and displacement data were converted to stress and strain respectively, and a tensile stress-strain curve was constructed. The stress was calculated by dividing the load with the cross-sectional area of the specimen. The strain was obtained as the ratio of the measured motion of the cross-heads to the initial gauge length of the specimen.

For more detailed description of the technique and results on other material systems see [1-5].

6.2.2 Results

The room temperature test results for the various lay-ups are shown in Fig.5. Since the loading capacity is limited to 1000lbs, (in practice to 700-800lbs.), only the 8-ply specimens were tested. Even though there is some scattering in the results obtained for 4 different specimens, the tensile stress-strain curves (Fig.5), as expected, are first linear, and later non-linear due to fiber breaking and interfacial debonding. This is also documented in microphotographs (a)-(d) of Fig.6. The $[0^0]_{8\text{-ply}}$ specimen has as expected the highest strength of approximately 1400 MPa. The failure strength is reduced for other lay-up configurations dropping to approximately 800 MPa for the $[0^0/90^0/0^0/90^0]_s$ specimens, to 300 MPa for the $[0^0/+45^0/90^0/-45^0]_s$ specimens and finally to approximately 90 MPa for the $[+45^0/-45^0/+45^0/-45^0]_s$ specimens, as can be seen in Fig.5. It must also be noted that, the failure strain is almost the same (4.5%) for all configurations except for the $[+45^0/-45^0/+45^0/-45^0]_s$ where it drops to approximately 2%. This can be easily explained considering the fact that the failure mode was different for the various configurations. For example, as stated earlier, the $[0^0]_{8\text{-ply}}$ specimens failed largely due to interfacial debonding and fiber breaking. When a fiber breaks, usually there is large stress concentration (both shear and normal stress) at that location. This may lead to separation of fiber matrix interface, and usually is referred to as interfacial debonding. If the interfacial normal stress is tensile, then there will be opening of the fiber/matrix interface. Due to shear there is slippage between fiber and matrix, but is much less visible. On the other hand the $[+45^0/-45^0/+45^0/-45^0]_s$ specimens failed at $\pm 45^0$ along the fiber/matrix interface as shown in Fig.7. When subjected to uniaxial testing, the maximum shear stress occurs at 45^0 with the loading direction. In the case of $\{+45^0/-45^0\}$ specimens this is parallel to the fiber directions. Thus the specimens fail due to maximum shear stress which occurs along the fiber/matrix interface. Thus the very high failure strains observed for the configurations other than $\{\pm 45^0\}_{2s}$ specimens can be attributed to fiber pull-out which occurred after fiber breakage. Excluding fiber pull-out, the failure strain would be less than 2%. This also explains the lower failure strain, less than 2%, obtained for the $\{\pm 45^0\}_{2s}$ laminates. Next the high temperature testing was started. First $[0^0]_{8\text{-ply}}$ and $[+45^0/-45^0/+45^0/-45^0]_s$ specimens were subjected to tensile load and 125^0C. The stress-strain curves for these cases and their room temperature counterparts are shown in Figs. 8 and 9. It is seen that there is a significant decrease in failure strength due to higher temperature. At this point the tensile/heating substage broke down and was sent to repair. Thus the remaining high temperature testing will be completed during the option years, as soon as the equipment is received from repair. It must be noted that no matrix cracks were observed during testing. This fact may be attributed to the higher toughness of the matrix.

6.2.3 Discussion and Conclusions

The tensile testing in SEM has provided us extremely important information about the mechanical behavior of the composite at room and elevated temperatures. The results are summarized in Fig. 5, 8 and 9. Fig. 5 shows the effect of various lay-up configurations. It is noted that the strength, stiffness and failure strain are greatly affected. Using the rule of mixtures, transformation formulas and classical lamination theory, one can predict the stiffness of the composite for the various configurations. Comparison of the predicted values with experimental data is given in Table 3. It must be noted the agreement between theoretical and experimental values is very good. The failure strength also is affected by the lay-up configuration. In this case the simulation of experimental results is done through the Finite Element model which is discussed later.

The SEM high temperature results are limited because the testing is continuing during Phase II of the project. But from the limited data obtained before the equipment broke down, it appears that the strength of the composite significantly decreases with increasing temperature.

For this part of project the following conclusions can be drawn:

- The stress-strain curve is first linear and then non-linear; the non-linear portion is due to damage in the composite.
- The lay-up configuration can greatly affect the strength, stiffness, failure strain and failure mode of the composite.
- Because the matrix is a toughened epoxy no matrix cracks were observed.
- The stiffness of the composite can be predicted using the rule of mixtures, transformation formulas and the classical lamination theory.
- The strength of the material decreases with increasing temperature.

6.3 TESTING IN MTS

6.3.1 Description of Experiments

The dog-bone shaped composite specimens were also tested in a MTS machine both at room temperature and 75^{0}C and 125^{0}C. The composite specimens were placed in the MTS machine using special grips. The tensile experiment is displacement controlled, meaning that the maximum displacement is set and the load is increased until the specimen breaks. The applied force and displacement were read by proper conversion of the recorded voltage. Stresses were calculated by dividing the applied force with the cross-section of the specimen, and strains were obtained by dividing the displacement with the gauge length of the specimen. For high temperature testing the specimen was placed in the environmental chamber and tested at the desired temperature.

6.3.2 Results

The results at room temperature for $[0^0]_{24\text{-ply}}$ (type 2), and $[0^0/0^0/90^0/90^0/0^0/0^0/90^0/90^0/0^0/0^0/90^0/90^0]_s$, $[0^0/0^0/0^0/+45^0/+45^0/+45^0/90^0/90^0/90^0/-45^0/-45^0/-45^0]_s$ and $[+45^0/+45^0/-45^0/-45^0/+45^0/+45^0/-45^0/-45^0/+45^0/+45^0/-45^0/-45^0]_s$ are summarized in Fig. 10. For each lay-up at least 4 specimens were tested, and the results look quite consistent, without significant scattering. For all configurations, the stress-strain curve

has a linear portion corresponding to the undamaged state, followed by a non-linear portion corresponding to the damaged state. The shape of the non-linear portion varies with the various lay-up configurations which have different failure modes. The effect of lay-up configuration can be clearly seen in Fig.10, where the results for the four different configurations are plotted together. As expected the $[0^0]_{24\text{-ply}}$ specimens have the highest strength, which decreases significantly for the other configurations. Indeed, the ultimate strength of the $[+45^0/+45^0/-45^0/-45^0/+45^0/+45^0/-45^0/-45^0/+45^0/+45^0/-45^0/-45^0]_s$ specimen is only 11% of that for the $[0^0]_{24\text{-ply}}$ specimen. The stiffness also decreases in the same order from the highest value for the $[0^0]_{24\text{-ply}}$ to the lowest value for $[+45^0/+45^0/-45^0/-45^0/+45^0/+45^0/-45^0/-45^0/+45^0/+45^0/-45^0/-45^0]_s$. The strain at failure on the other hand decrease in the same order except for the $[+45^0/+45^0/-45^0/-45^0/+45^0/+45^0/-45^0/-45^0/+45^0/+45^0/-45^0/-45^0]_s$ specimens where it increases significantly. This may be due to the large strain produced during shear failure. In the $\pm 45^0$ specimens the failure was slippage along the fiber/matrix interface at 45^0 which may have produced large strains in the loading direction. The variation of the stiffness and strength with configuration is summarized in Table 4. The same specimens were also tested at 75^0C and 125^0C using the environmental chamber of the MTS machine. The results at 75^0C are shown in Fig.11, and at 125^0C are plotted in Fig.12. At elevated temperatures the basic shape of the stress-strain curves did not change and the tensile damage behavior was similar. This can be clearly seen by examining Figs. 11 and 12, which summarize the results for the 4 configurations at 75^0C and 125^0C respectively. On the other hand temperature has a significant effect on the strength and stiffness of the composite. The strain at failure does not appear to be affected much by temperature. To show the temperature effect, for each lay-up configuration the stress-strain curve is plotted at various temperatures in Figs. 13-16. It is seen that the ultimate strength and the stiffness decrease with increasing temperature. For example for the $[0^0]_{24\text{-ply}}$ specimen, the ultimate strength of approximately 975 MPa is reduced to 760 MPa at 125^0C, a decrease of 22%. The only exception appears to be for the $[0^0/0^0/0^0/+45^0/+45^0/+45^0/90^0/90^0/90^0/-45^0/-45^0/-45^0]_s$ specimens where the temperature effect is more ambiguous (Fig. 15). The reduction in stiffness and strength due to temperature usually is attributed to the change in the properties of the epoxy and has been observed for many epoxy matrix systems. The ambiguity of the results for the $[0^0/0^0/0^0/+45^0/+45^0/+45^0/90^0/90^0/90^0/-45^0/-45^0/-45^0]_s$ may be due to configuration.

6.3.3 Short Specimen Testing

Tensile testing was also conducted on shorter 16-ply specimens with the following configurations:

$[0^0/0^0/90^0/90^0/0^0/0^0/90^0/90^0]_s$,

$[0^0/0^0/+45^0/+45^0/90^0/90^0/-45^0/-45^0/]_s$ and

$[+45^0/+45^0/-45^0/-45^0/+45^0/+45^0/-45^0/-45^0]_s$.

The main reason of conducting these tests was to ascertain whether the size of the specimens had any effect on the behavior of the composite. The results at room temperature, 75^0C and 125^0C are shown in Figs.17-19, and basically conform with those obtained for longer specimens. It must be noted that, the same configuration and temperature effects on the failure strength, stiffness and strain at failure are observed here also. The effects of configuration on strength, stiffness and failure strain of the composite at various temperatures were shown in Figs. 17-19. Figs. 20-22 depict the effect of temperature for three different lay-up configurations.

6.3.4 Discussion and Conclusions

From the MTS testing tensile testing results described above much was learned about the mechanical behavior of S2glass/toughened epoxy, especially about strength, stiffness, failure strain and temperature dependence. Our conclusions can be summarized as follows:

- The stress-strain curves are first linear, then become non-linear due to fiber breaking, interfacial debonding between matrix and fiber and interlaminar damage.
- Strength and stiffness of composite vary considerably with lay-up configuration, with the uniaxial specimen exhibiting, as expected, the highest strength and stiffness.
- The strength and stiffness of the composite decrease with increasing temperature.
- No matrix cracks were observed due to the use of toughened epoxy.
- For tensile testing, size effect was negligible on mechanical properties of the composite.

6.3.5 Comparison of SEM and MTS Results

One of the reasons of carrying out tensile experiments both in SEM and MTS was to ascertain whether one could obtain the same results using different techniques and specimen dimensions.

The results for SEM were summarized in Fig. 5, while those for MTS were given in Fig 10. First it is observed the behavior obtained from both testing is quite similar. However the strength and stiffness obtained from MTS testing were somewhat lower. The reason for this is that the SEM and MTS specimens came from different batches and the volume fraction of fiber for MTS specimens was less than the nominal 55% assumed, and thus an explanation for the lower strength obtained in MTS testing.

6.4 THE THREE-POINT BENDING TESTS IN MTS

6.4.1 Description of experiments

The same S2 glass/toughened epoxy composite was also tested under 3-point bending loading at room and higher temperatures. In this case the specimens were rectangular coupons of various configurations, dimensions of which are given in Fig. 3.

The test set-up is shown schematically in Fig.23. In this case, the mid-span displacement was plotted vs. the bottom mid-span stress which was approximately calculated from ($\sigma = \frac{Mc}{I}$). The min-span displacement was measured through the motion of the cross-head of the MTS machine. In the formula M=PL/4, the moment of inertia is calculated using an equivalent cross-section with uniform stiffness properties. The room temperature tests were carried out for both Type 2 and Type 1 specimens. Type 2 specimens were also tested at higher temperatures namely 75^{0}C and 125^{0}C.

6.4.2 Results

The room and elevated temperature results are presented in Figs. 24-30. In Figs. 24-27 the mid-span normalized stresses are plotted vs. the mid-span normalized displacements at room temperature, 75^{0}C and 125^{0}C to show the effect of lay-up configurations on the behavior of the composite. The three-point bending behavior of this composite is mostly linear, followed by a sudden drop in the stress indicating failure of at least one ply or delamination. Ply failure is usually associated with broken fibers and severe

damage in the ply. Delamination, on the hand is the separation of the laminae due to either high shear or tensile interlaminar stresses. This sudden drop is seen almost in all the curves obtained, except for the $[+45^0/+45^0/-45^0/-45^0/+45^0/+45^0/-45^0/-45^0/+45^0/+45^0/-45^0/-45^0]_s$ specimen, where the drop is more graduated. The stress obtained for Type 2 specimens were slightly higher. The effect of high temperature is depicted in Figs. 27-29. The general trend of the curves is similar to that obtained for testing at room temperature. However there is a significant drop in the ultimate strength of the composite with increasing temperature. There is a slight decrease in the stiffness due to higher temperatures.

6.4.3 Discussion and Conclusions

Again it is observed that both the lay-up configurations and temperature have a significant effect on the mechanical behavior of the composite. The bending strength is reached when a ply fails or delamination occurs. This behavior was not observed for the [±45] laminates. Temperature effect on stiffness was slight but very significant on strength, resulting in lower strength at higher temperatures. The conclusions for 3-point bending can be summarized as follows:

- Bending strength is reached due to ply failure or interlaminar delamination.
- Lay-up configuration has a significant effect on bending strength and stiffness of composite, with significantly lower values obtained for $[\pm 45^0]$ laminates.
- The temperature effect was slight on bending stiffness, but much more pronounced on bending strength. Bending strength usually decreased with increasing temperature.

6.5 INTERFEROMETRIC STRAIN DISPLACEMENT GAUGE

6.5.1 Experiment

We proposed to use an interferometric strain measurement technique to analyze the strain on toughened polymeric composite materials (S2 glass/ toughened epoxy) at room and elevated temperatures (i.e. up to 125^0 C).

Much of the early work using this optical method of measuring strain and displacement was done by Guillot and W. N. Sharp Jr [6-10]. By measuring interferometrically the relative displacement of two reflecting indentations in a specimen the local strain can be determined. The advantages of this method are:

- A short gauge length (0.125 mm).
- No electrical or mechanical contact with the sample.
- No temperature sensitivity.
- A relatively easy experimental technique.

6.5.1.1 Interference Fringe Pattern

When monochromatic light is incident upon a small surface (the order of the wavelength of light) a reflection diffraction pattern is formed.

If two grooves are placed close together, an interference pattern is formed by the two overlapping diffraction patterns if the incident monochromatic light is coherent. The position of the interference minima are given by

$$\sin\theta = (\lambda/d) (m + 1/2), \quad m = 0, +/- 1, +/- 2.... \tag{1}$$

The fringe spacing is determined by differentiating Eq. (1) with respect to m and setting $\Delta m = 1$, i.e.

$$\Delta\theta = \lambda/(d \cos\theta) \tag{2}$$

where, d is the distance between grooves, λ is the wavelength of light, and θ is the angle measured from the incident beam to the reflected beam. Closer spaced grooves generate wider spaced fringes and vice versa.

6.5.1.2 Strain Measurement

The strain on a surface can be determined by measuring the change in the location of the interference fringes as the distance between the two grooves vary. If the observation position is fixed, $\theta = \alpha$, the change in distance between the two grooves from Eq. 1, δd, is

$$\delta d = (\lambda \, \delta m)/\sin\alpha \tag{3}$$

where δm is the variation in fringe order at the observation position. The way in which the value of δm is determined depends on the range of the strain. For large strain (strain > 1%) δm is obtained by counting the number of fringes (i.e. maxima and minima) passing the observation point. For small strain δm is determined by tracking one fringe (maxima or minima) and measuring its displacement from the observation point and dividing the displacement by the fringe spacing.

Some of the fringe motion is due to the rigid body motion of the sample rather than the strain in the specimen. The motion parallel to the gage can be eliminated by averaging the two fringe patterns reflected from the two grooves in the sample. Hence, in practice the strain is determined from

$$\varepsilon = \delta d/d_0 = ((\delta m_1 + \delta m_2)/2) (\lambda / (d_0 \sin\alpha_0)) \tag{4}$$

where d_0 is the original groove spacing.

6.5.1.3 Experimental Technique

Illustrated in Fig. 31. is a schematic of the general IDSG setup, while Fig. 32. is a photograph of the actual experimental set-up used for 3-point bending measurements. Two very small indentations, as shown in Fig. 33, are placed approximately 100 μm apart on the sample surface with a Vicker's hardness tester. The depth of the indentations is approximately 25 μm. The specimen is placed inside a testing unit. When the indentations are illuminated with a laser, interference fringe patterns, shown in Fig. 34., are produced due to the path differences between the light rays reflected from the sides of the two marks. The relative displacement between the two points is proportional to the motion of the fringes. Fringe motion is monitored in real time by two photodetectors. The face of the photodetector is masked by a thin slit which

is narrower than the spacing between the fringes and is also covered with an interference filter to block out background light. The computer calculates a value for the local strain from the displacement measurements. This setup can be referred to as the interferometric displacement strain gauge (ISDG).

6.5.2 Results

6.5.2.1 Three Point Bending

To test the ISDG set-up three-point bending measurements were performed on aluminum samples using a standard Machine Testing System (MTS) unit. Outboard equipment for the MTS monitored the load, load rate and displacement of the jaws of the MTS. The aluminum sample was prepared with two indentations 100μm apart (gauge length). The indentations were illuminated with a 35 mW Helium Neon laser producing bright interference fringes which were monitored with slit covered silicon PIN diodes. The output of the PIN diodes were connected to an analog to digital converter and then to a computer where its values were plotted as a function of time, as illustrated in Fig. 35. As the measurement is executed and the sample bends, the spacing between the two indentations change causing the fringe (interference) pattern to move across the slits covering the photodetectors which record the fringe signal as a function of time and load. This information is converted into a strain vs. time plot as shown in Fig. 36. We compared the ISDG measurements with the theoretical MTS curve.

6.5.3 Conclusions

We have demonstrated the feasibility of using IDSG for 3-point bending measurements. This conclusion is supported by the strong correlation between the IDSG and standard MTS curves illustrated in Fig. 36. Our preliminary study has been for aluminum samples. This technique can be applied also to composite materials, which are non-reflective normally, by bonding aluminum sheets to the composite material with epoxy. This will be accomplished during the next phase of the project.

6.6 THE MICOSTRUCTURAL MODEL AND THE FINITE ELEMENT RESULTS

6.6.1 Description of the Model

In this section we introduce the model developed to explain and simulate the observed behavior of the composite under testing. The model is based on micromechanics and finite element calculations. Obviously the easiest specimens to model are the uniaxial ($[0^0]_{8\text{-ply}}$) specimens subjected to tensile loads at room temperature. When there is no damage in the composite, the stress-strain curve is linear and the stiffness of the composite can be theoretically predicted using the law of mixtures. Indeed the slope of the stress-strain curve calculated using the law of mixtures, as expected matches the experimental results extremely well (Fig.39). The challenge is to match the non-linear portion of the curve. It is well known that the non-linearity in the stress-strain curve is due to damage in the composite. As observed in the SEM for the $[0^0]_{8\text{-ply}}$ specimens, this damage consists mostly of interfacial debonding between matrix and fiber and fiber breaking. The model thus consists of a fiber surrounded by matrix and two fibers (3-fiber model) or matrix and four fibers (5-fibers model) with the rest of the composite represented by a homogeneous medium where the properties have been smeared out. Damage is introduced through fiber break and an interfacial crack between fiber and matrix, and it is assumed that there is a frictional shear stress (τ) at the fiber/matrix interface. The progression of damage is modeled through the propagation of the interfacial

crack and application of the energy criterion of fracture mechanics. The calculations were carried out using the finite element program ABAQUS. The model and the finite element mesh are shown in Figs. 37and 38.

6.6.2 Results and Discussion

The finite element results for various values of the frictional shear stress are compared with the experimental results in Fig. 39. The non-linear portion of the calculated stress-strain curve varies with the frictional shear stress. It is seen that, with the appropriate selection of the interfacial frictional shear stress, the model can simulate the experimental data extremely well. For the example given in Fig. 36 the best fit with experimental data is obtained for $\tau = 30$MPa.

6.6.3 Conclusion

It is concluded that the Finite Element model described above can be used to simulate the experimental results with an appropriate selection of the interfacial frictional shear stress.

7 References

1. B.M. Liaw, S.J. Zhang and F. Delale, "An Experimental Technique for Tensile Testing of Ceramic Matrix Composites in SEM at Elevated Temperature," *Advances in Experimental Mechanics and Biomimetics*, AD-Vol. 29/AMD-Vol. 146, ed. by W. F. Jones and J. M. Whitney, The American Society of Mechanical Engineers, New York, 1992, pp.1-12.

2. F. Delale, H.Q. Zhang, B.M. Liaw and S.J. Zhang "Tensile Damage Behavior of Ceramic Matrix Composites Under High Temperature," *Fracture and Damage*, AD-Vol. 27, ed. by A. Nagar, The American Society of Mechanical Engineers, New York, 1992, pp.103-108.

3. F. Delale, B.M. Liaw, S.J. Zhang and H.Q. Zhang "Tensile Behavior of Ceramic Matrix Composites at Room and Elevated Temperature," *Ceramic Matrix Composites and Other Systems*, ICCM/9, Vol. II, ed. by A. Miravete, *Proceedings of the Ninth International Conference on Composite Materials*, Madrid, Spain, 12-16 July, 1993, pp.55-62.

4. S.J. Zhang, H.Q. Zhang, F. Delale, B.M. Liaw, and J. H. Bode, "An Investigation of Tensile Damage Behavior of X5230/T800 Polymer Matrix Composites through in-situ Tensile Testing In SEM," *Proceeding of the American Society for Composites, 9th Technical Conference*, September 20-24,1994, University of Delaware, Newark, DE, pp.322-330.

5. S.J. Zhang, H.Q. Zhang, F. Delale, B.M. Liaw, and J. H. Bode, "Tensile Failure Mechanisms of Ceramic and Polymer Matrix Composites at Room and Elevated Temperatures," *Proceeding, Design and Performance of Composite Materials,* International Mechanical Engineering Congress and Exposition, Chicago, Illinois, November 6-11, 1994.

6. Guillot, M., "An Experimental Evaluation of Neuber's Cyclic Relation at Room and Elevated Temperature," Ph.D. dissertation, Louisiana Sate University, 1981

7. Sharpe, W. N., Jr. -Interferometric Surface Strain Measurement" Intl. J. Nondestructive Testing, Vol. 3, 1971, pp. 59-76

8. Guillot, M., "An Experimental Evaluation of Neuber's Cyclic Relation at Room and Elevated Temperature," Ph.D. dissertation, Louisiana Sate University, 1981

9. Sharpe, W. N., Jr. "Interferometric Surface Strain Measurement" Intl. J. Nondestructive Testing, Vol. 3, 1971, pp. 59-76

10. Sharpe, W. N., Jr. and Bohme, W., "Dynamic Fracture Toughness Measurements on Small Charpy Specimens - A Preliminary Study, The American Society for Testing and Materials, 1994, pp. 14 – 19

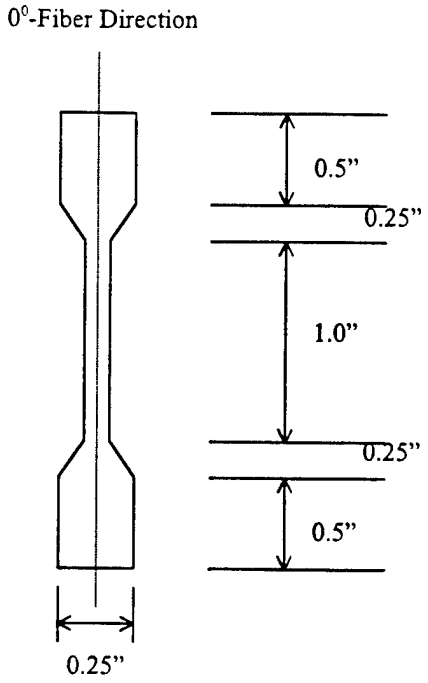

Fig.1 Specimen used in SEM testing

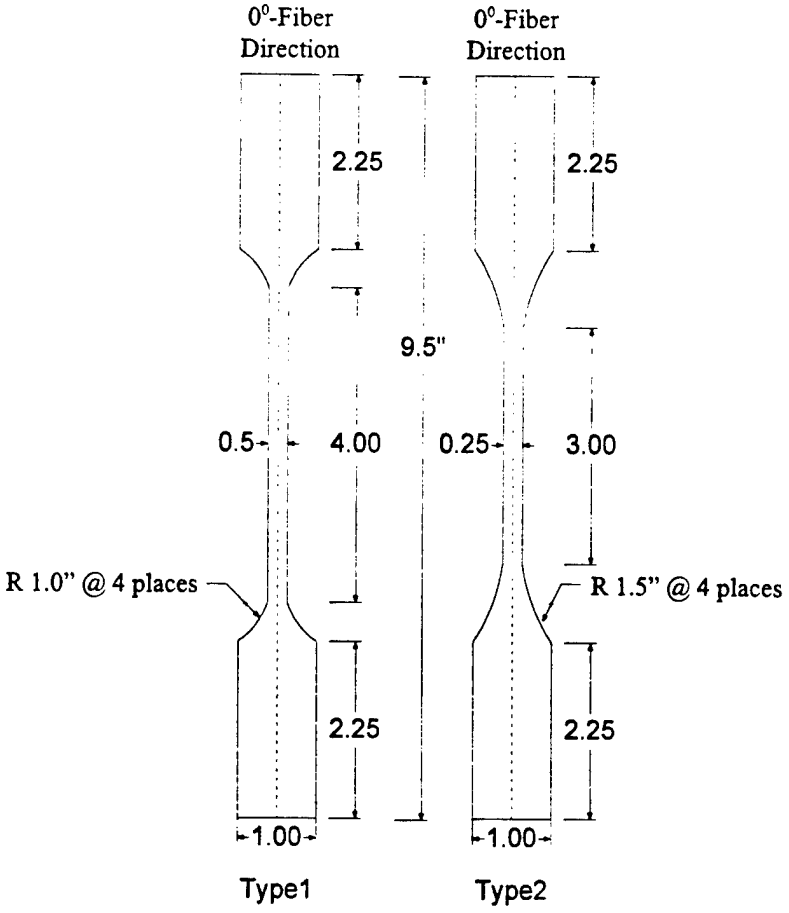

Fig.2 Specimens used in MTS tensile testing

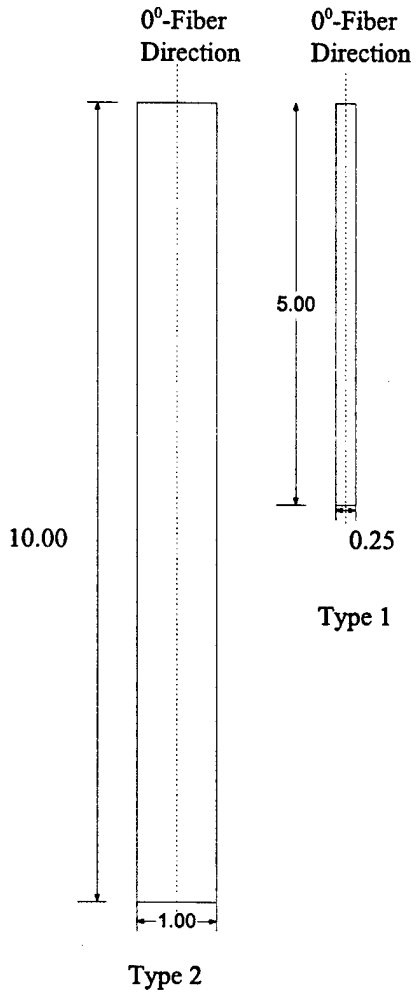

Fig.3 Specimens used in MTS 3-point bending tests.

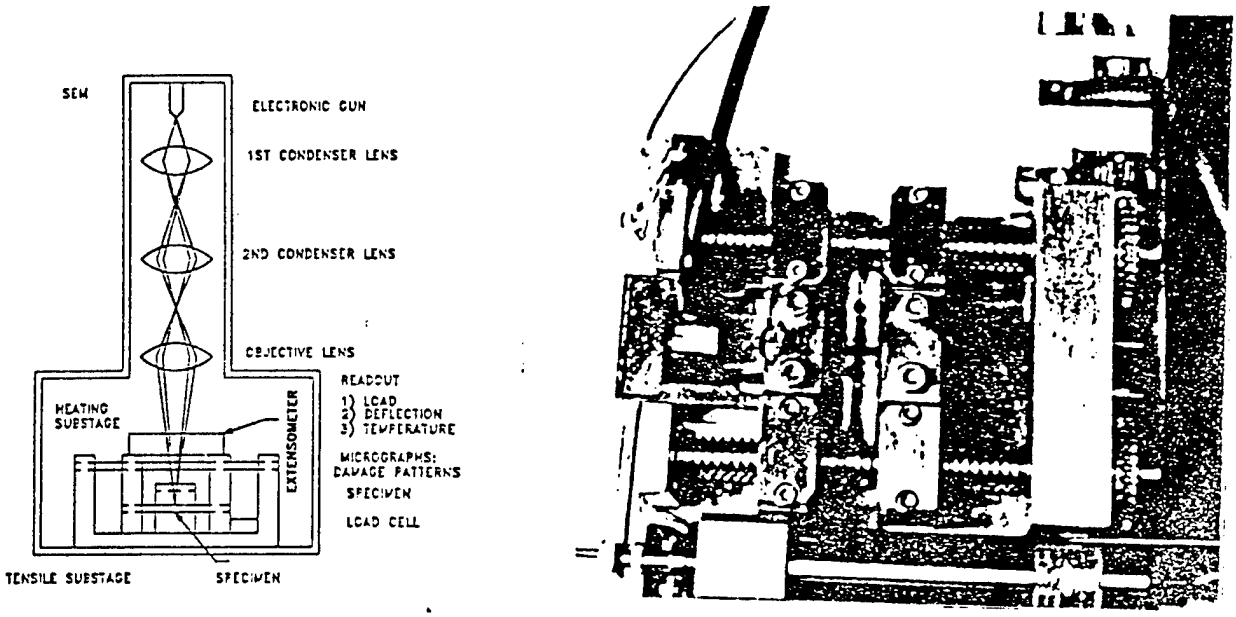

Fig.4 Experimental setup for in situ SEM damage observations and the assembly of tensile-heating substage.

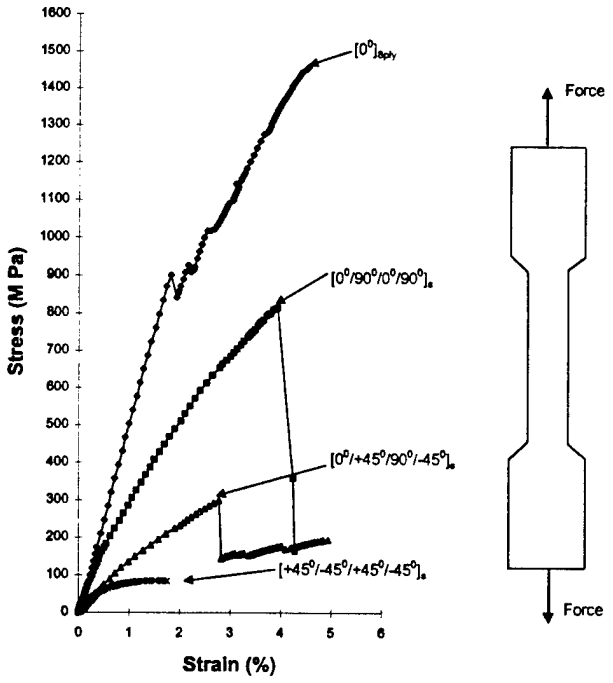

Fig.5 Comparison of strength for various lay-up configurations under tensile load at room temperature.

(a) No Load

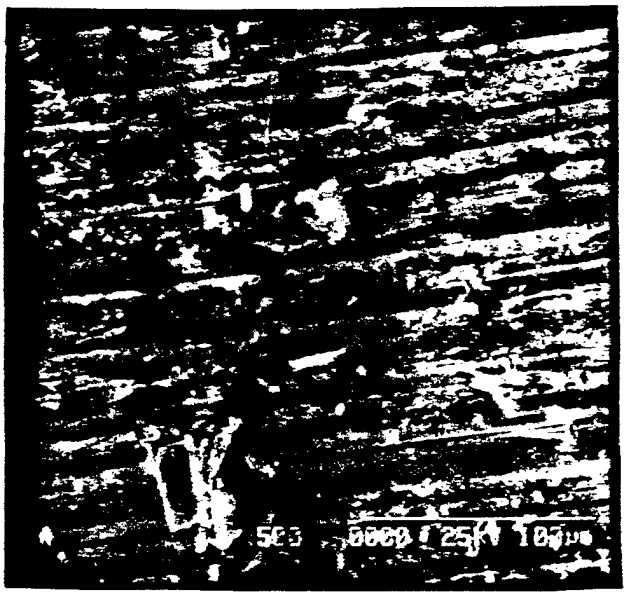

(b) at 930 MPa

(c) At 1300 MPa

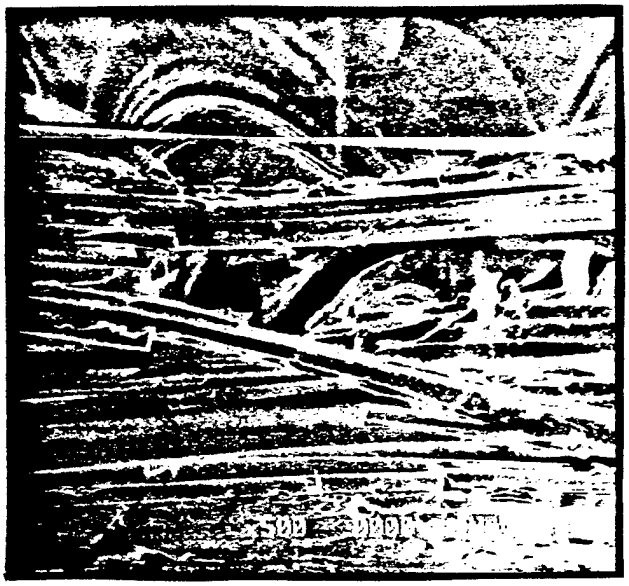

(d) at 1480 MPa
Fiber breakage

Fig.6 Microphotographs showing fiber breakage and interfacial debonding.

Fig.7 Composites failure at $\pm 45^0$ (at 80 MPa)

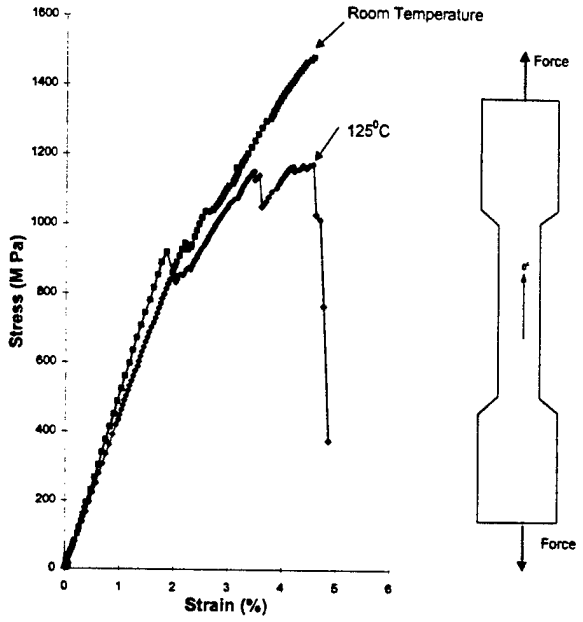

Fig.8 Comparison of room temperature and 125°C results for $[0^0]_{8\text{-ply}}$ specimens.

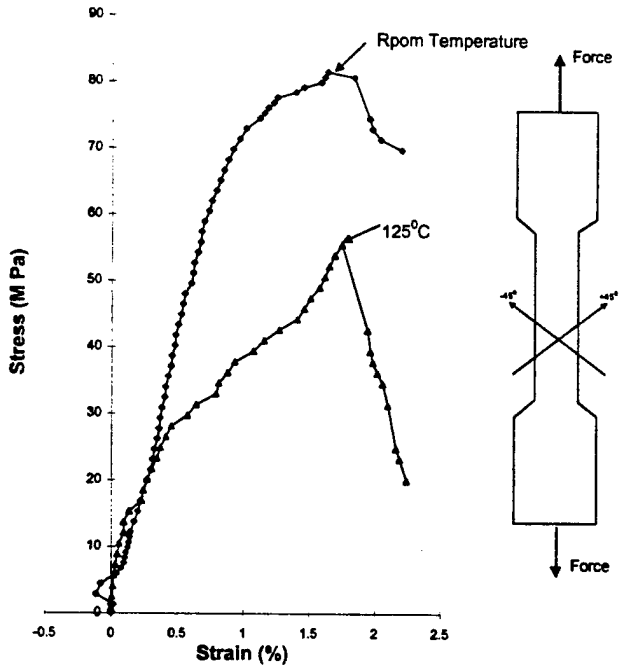

Fig.9 Comparison of room temperature and 125°C results for $[+45^0/-45^0/+45^0/-45^0]_s$ specimens.

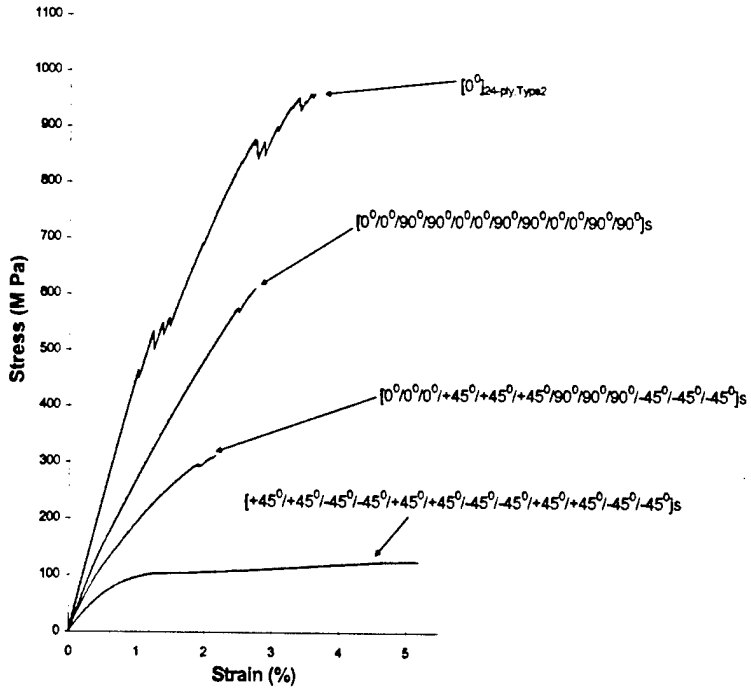

Fig.10 Comparison of MTS tensile results for various lay-up configurations at room temperature (Long specimens)

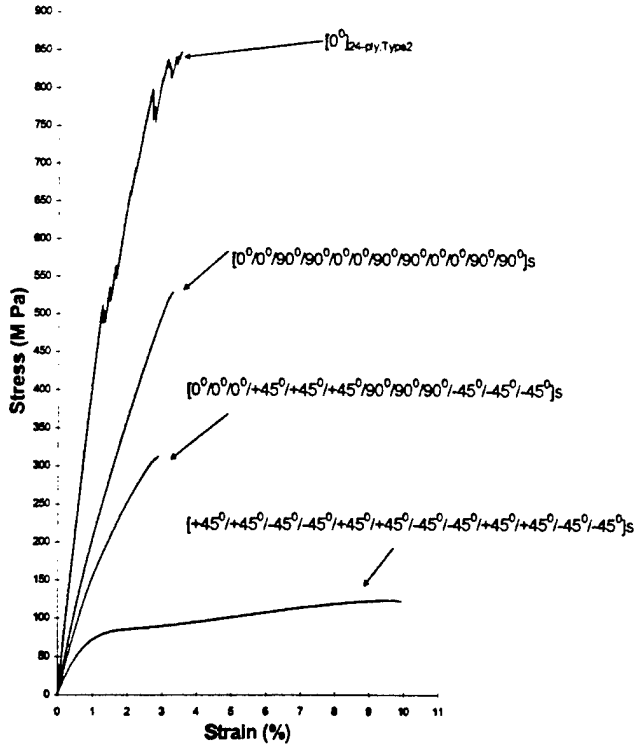

Fig.11 Comparison of tensile stress-strain curves at 75°C for various lay-up configurations (Long specimens)

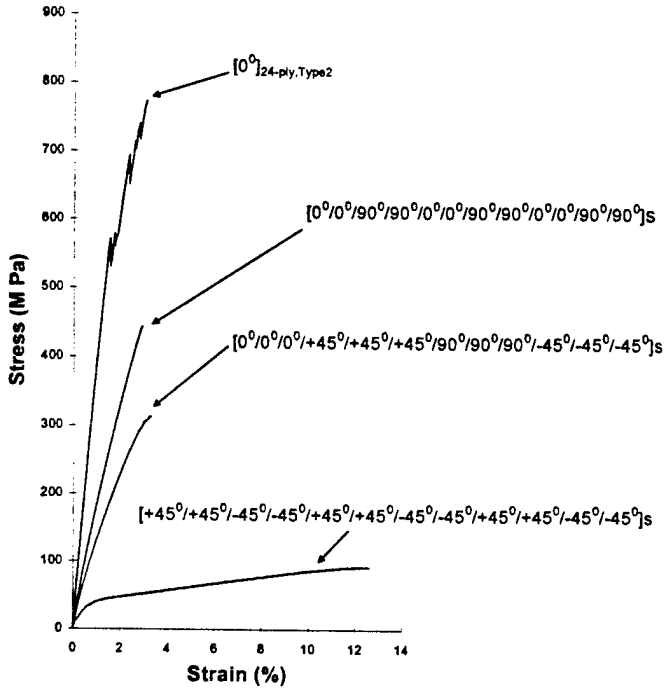

Fig.12 Comparison of tensile stress-strain curves at 125°C for various lay-up configurations (Long specimens)

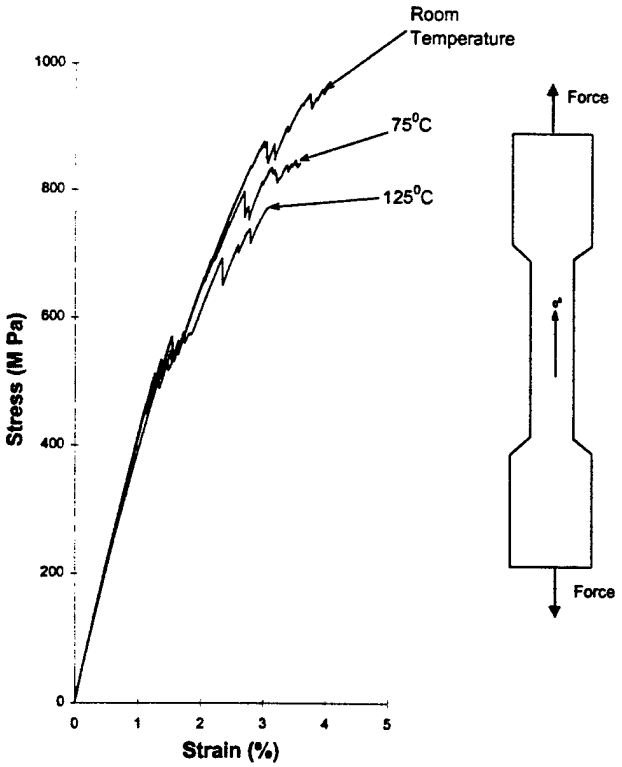

Fig.13 Effect of temperature on $[0^0]_{24\text{-ply, Type 2}}$ specimens

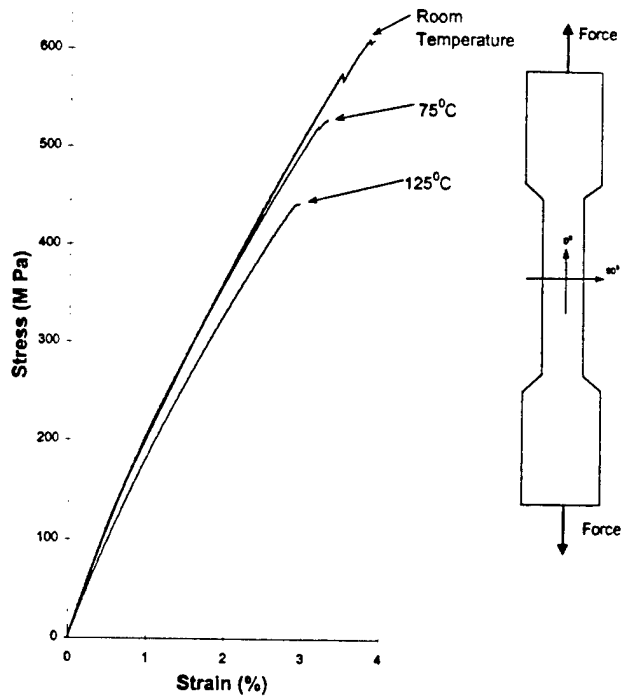

Fig.14 Effect of temperature on $[0^0/0^0/90^0/90^0/0^0/0^0/90^0/90^0/0^0/0^0/90^0/90^0]_s$ specimens

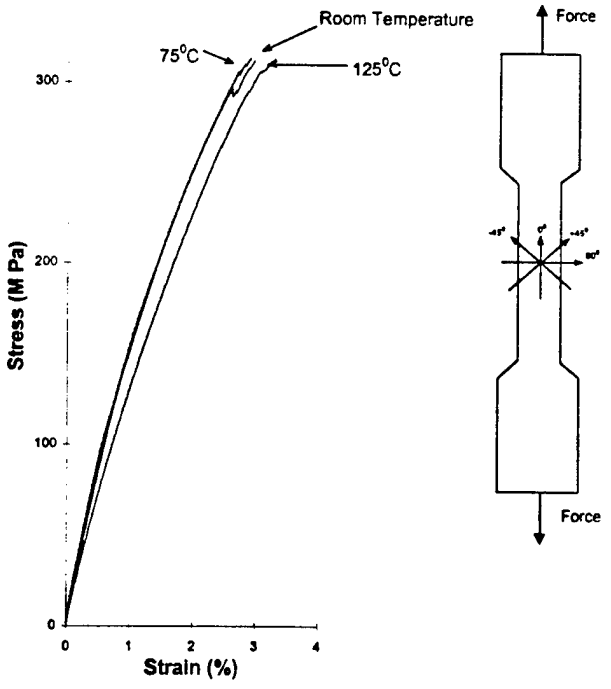

Fig.15 Effect of temperature on $[0^0_3/+45^0_3/90^0_3/-45^0_3]_s$ specimens

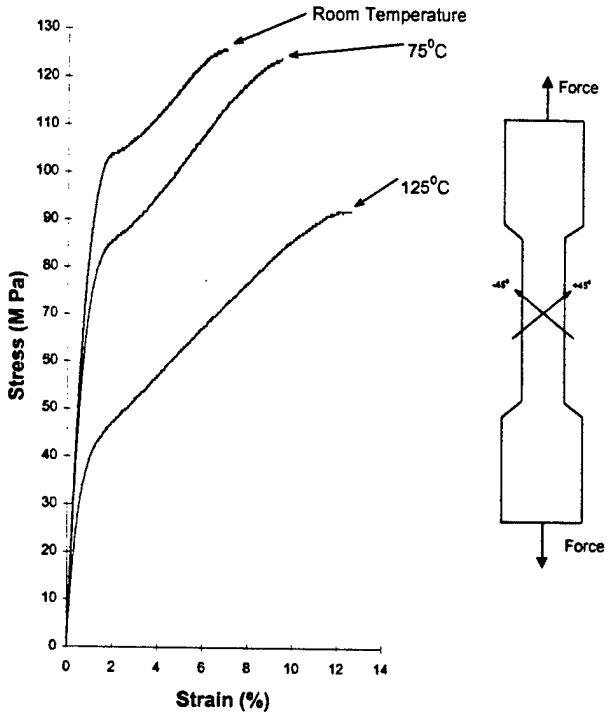

Fig.16 Effect of temperature on $[+45^0_3/-45^0_3]_{2s}$ specimens

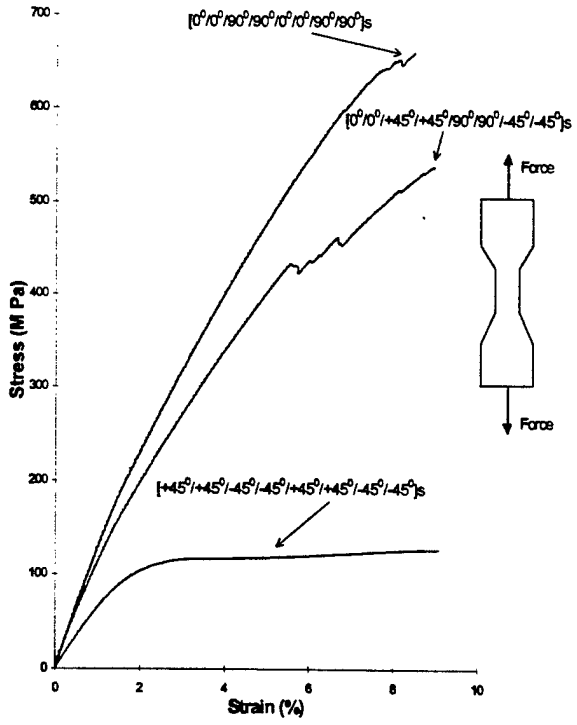

Fig.17 Effect of lay-up configuration at room temperature (Short specimens)

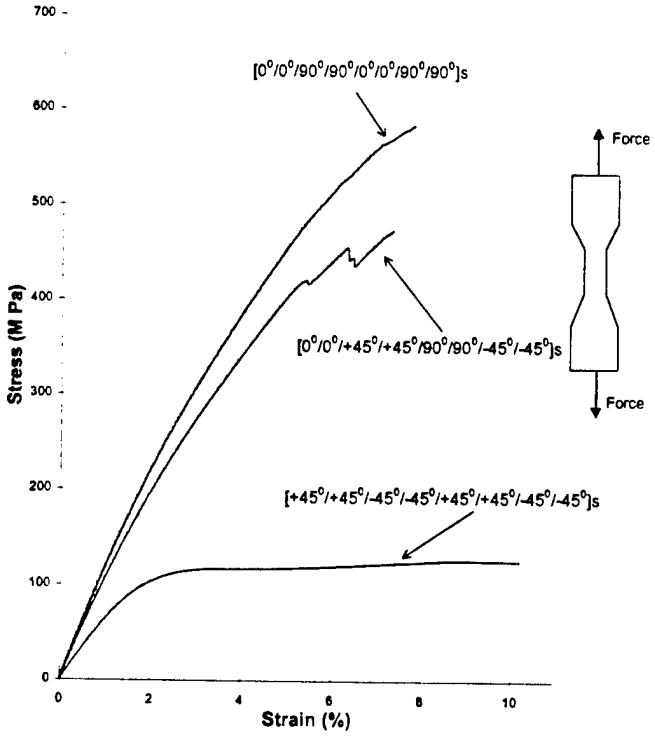

Fig.18 Effect of lay-up configuration at 75°C (Short specimens)

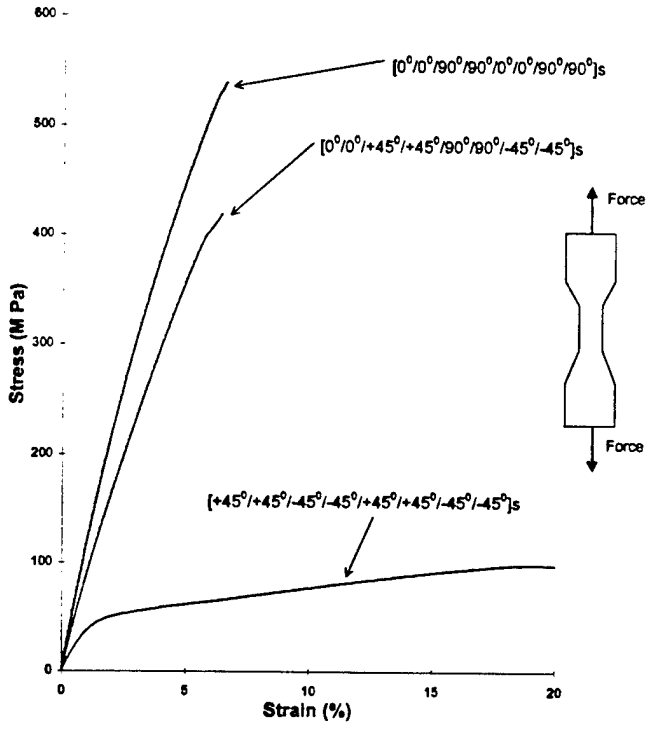

Fig.19 Effect of lay-up configuration at 125°C (Short specimens)

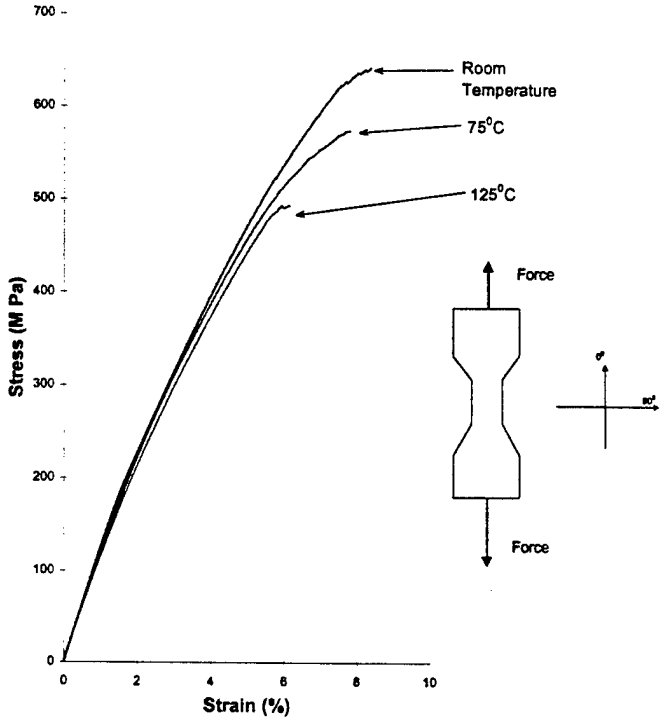

Fig.20 Effect of temperature on $[0^0/0^0/90^0/90^0/0^0/0^0/90^0/90^0]_s$ (Short specimens)

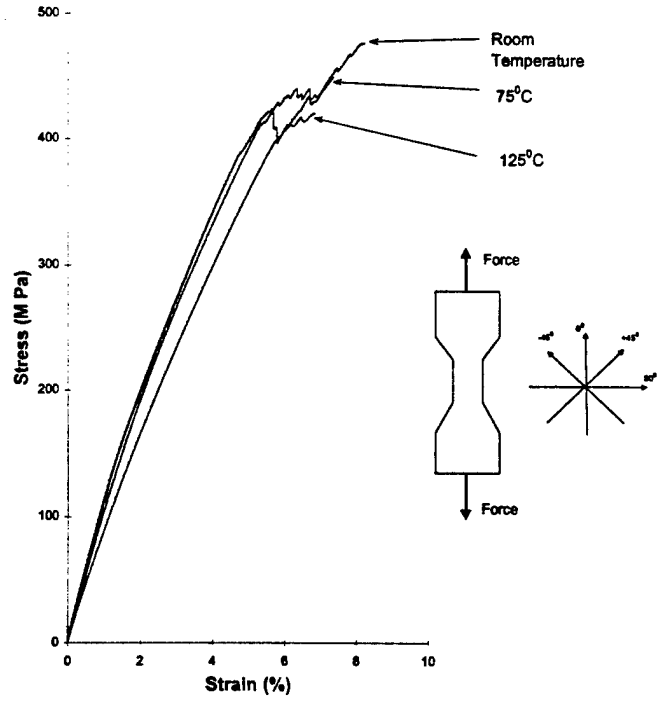

Fig.21 Effect of temperature on $[0^0/0^0/+45^0/+45^0/90^0/90^0/-45^0/-45^0]_s$ (Short specimens)

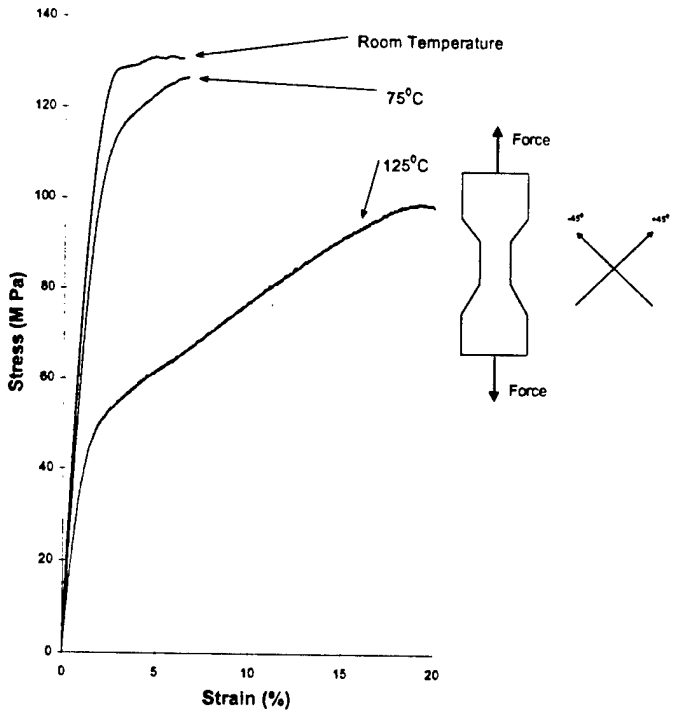

Fig.22 Effect of temperature on $[+45^0/+45^0/-45^0/-45^0/+45^0/+45^0/-45^0/-45^0]_s$ (Short specimens)

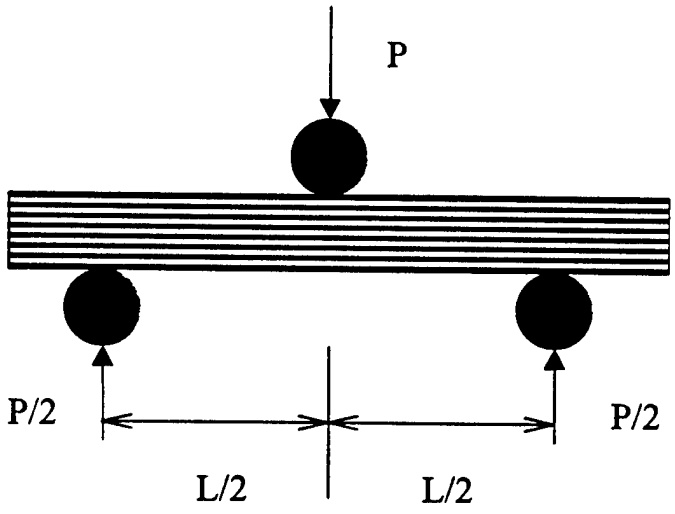

Fig.23 Three-Point Bending Test Set-Up

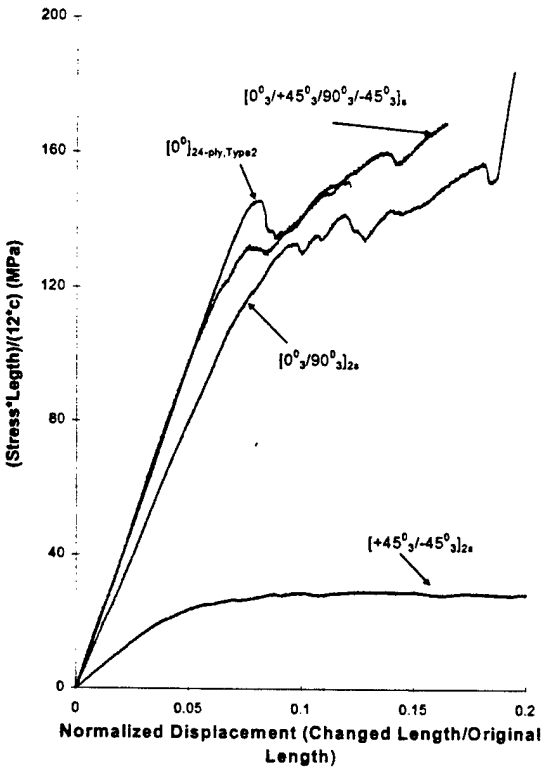

Fig.24 Effect of lay-up at room temperature (3-point bending)

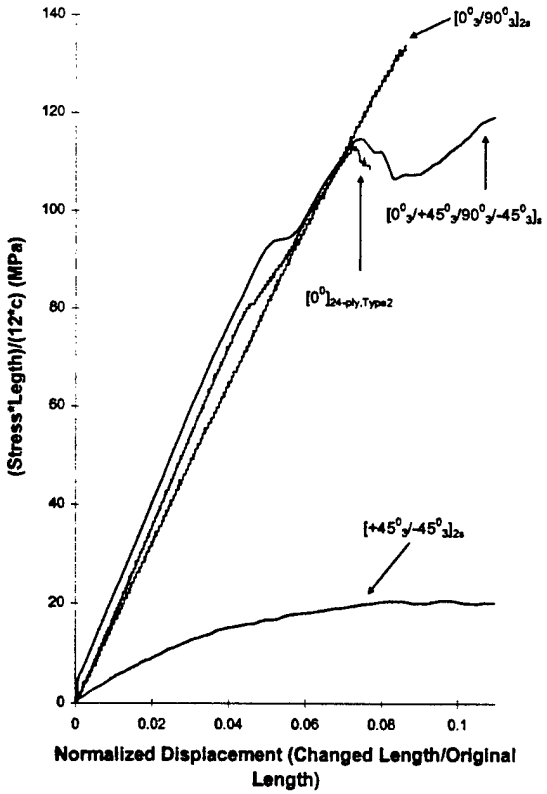

Fig.25 Effect of lay-up at 75°C temperature (3-point bending)

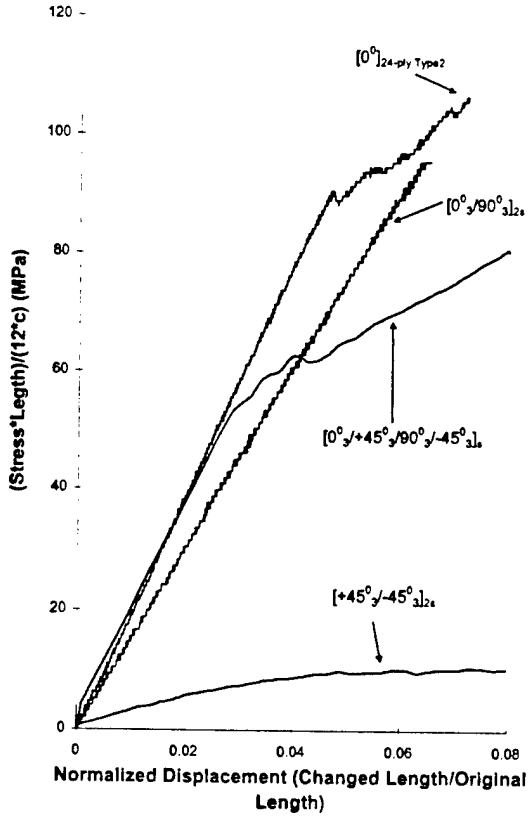

Fig.26 Effect of lay-up at 125°C temperature (3-point bending)

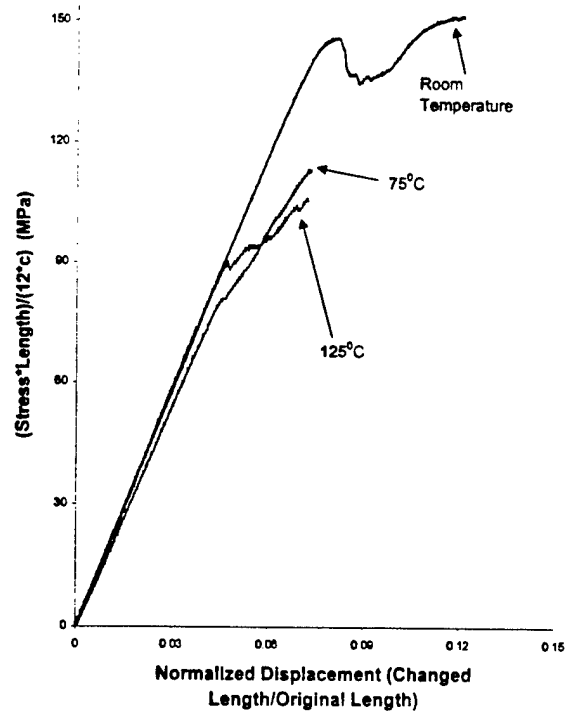

Fig.27 Effect of Temperature for $[0^0]_{24\text{-ply, type2}}$ (Three Point Bending)

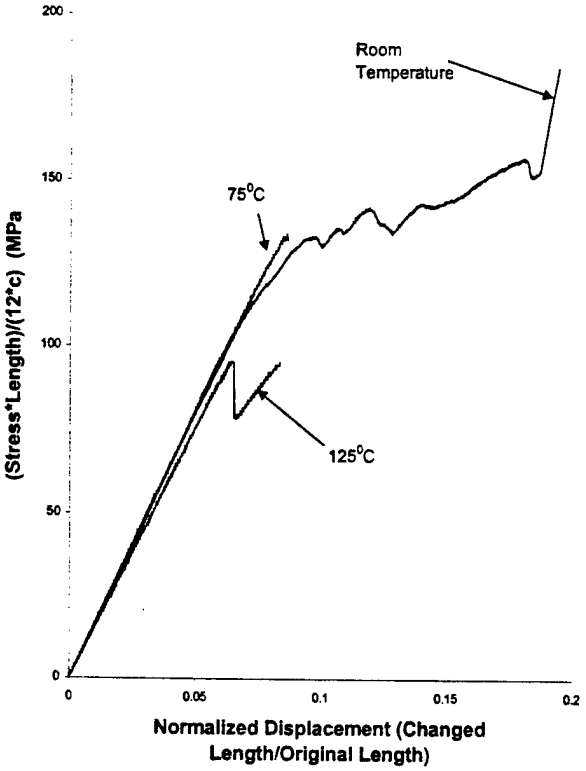

Fig.28 Effect of Temperature for $[0^0_3/90^0_3]_{2s,\ type2}$ (Three Point Bending)

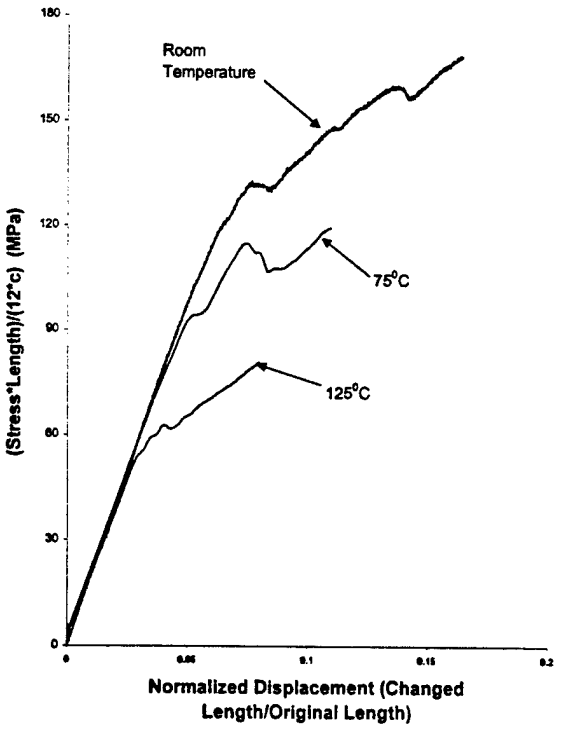

Fig. 29 Effect of Temperature for $[0^0_3/+45^0_3/90^0_3/-45^0_3]_{s,\ type2}$ (Three Point Bending)

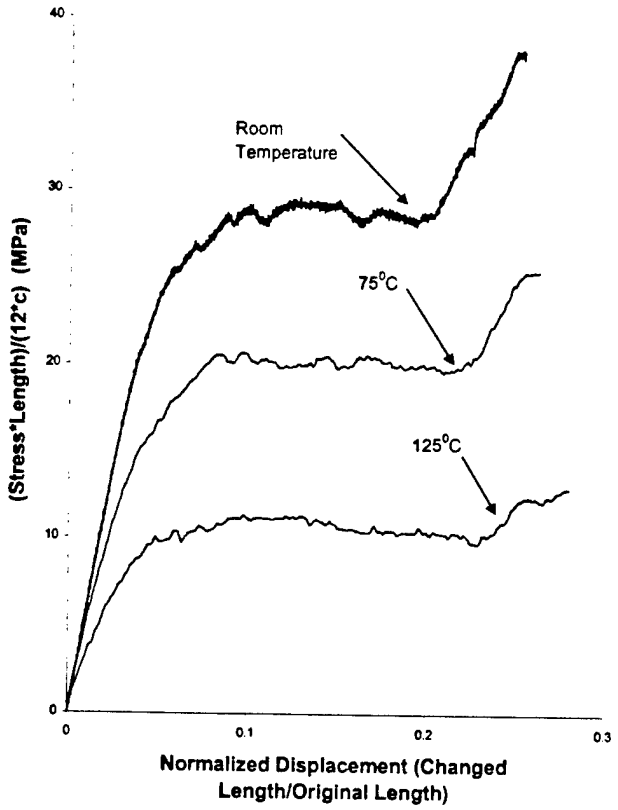

Fig.30 Effect of Temperature for $[+45^0_3/-45^0_3]_{2s,\ type2}$ (Three Point Bending)

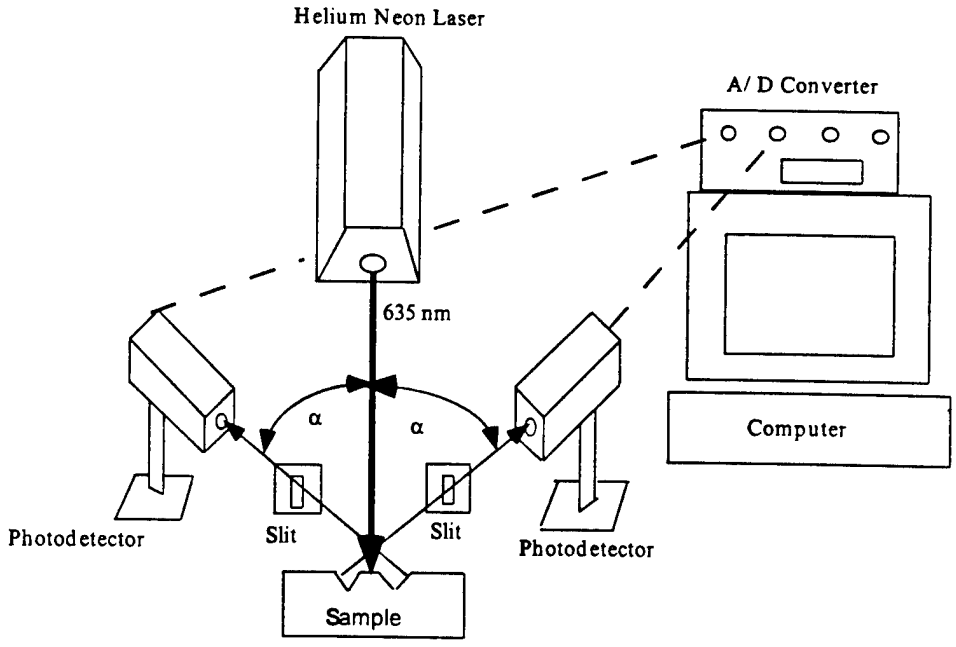

Fig.31 Schematic of interferometric strain displacement gauge (ISDG) setup.

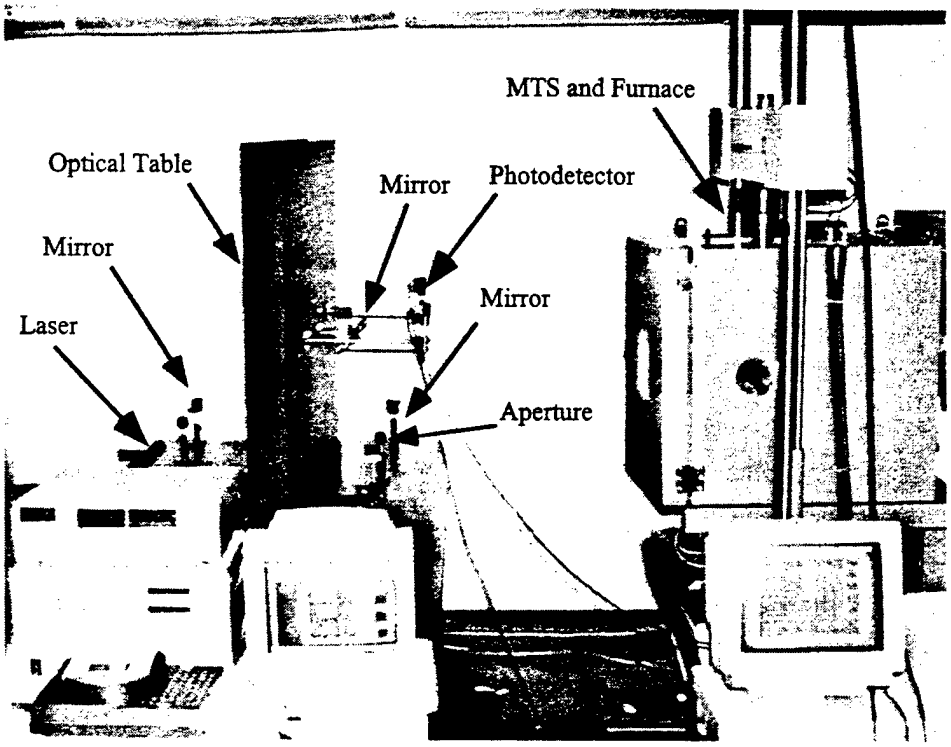

Fig.32 Photograph of the actual IDSG set-up used for the three-point bending measurements.

200X

Fig.33 A photograph of two indentations in S2-Glass/Toughened Epoxy Composites enlarged 200 times.

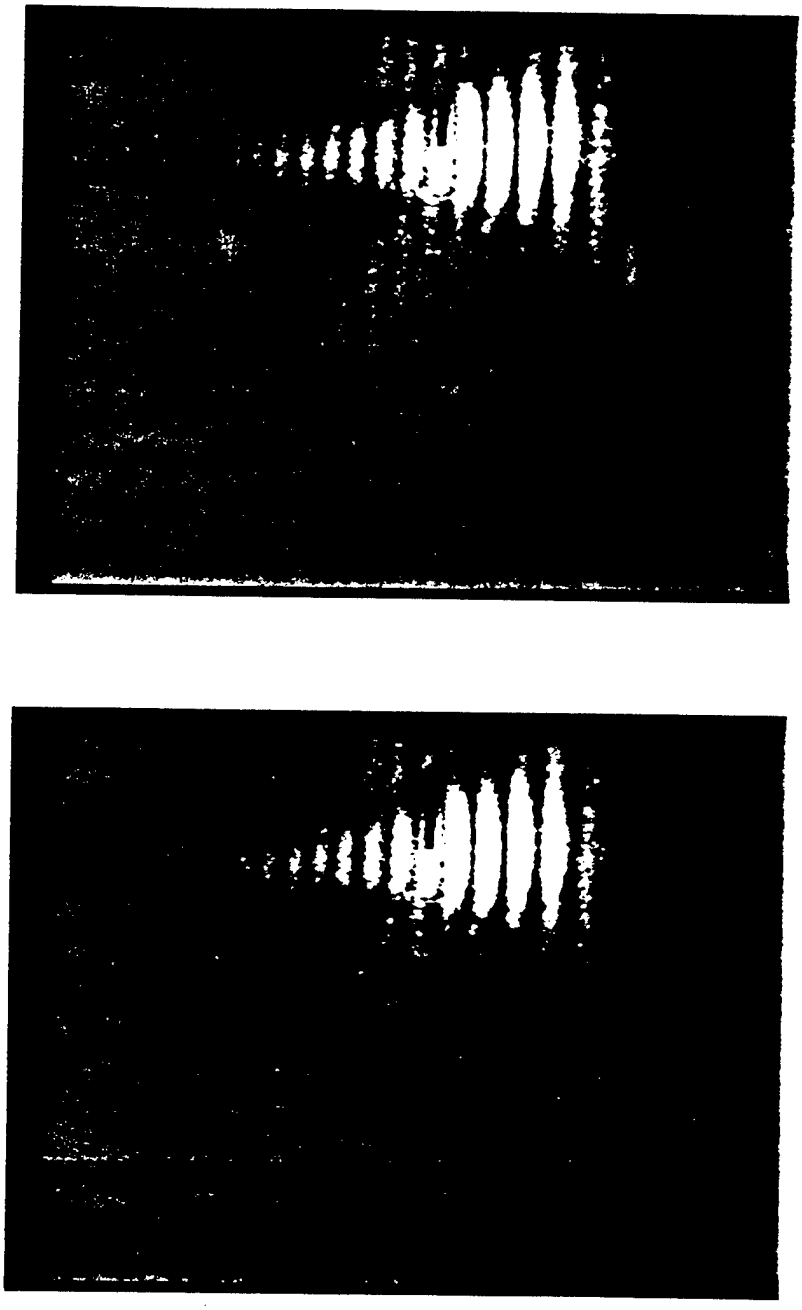

Fig.34 The Interference pattern from two indentations in an aluminum sample.

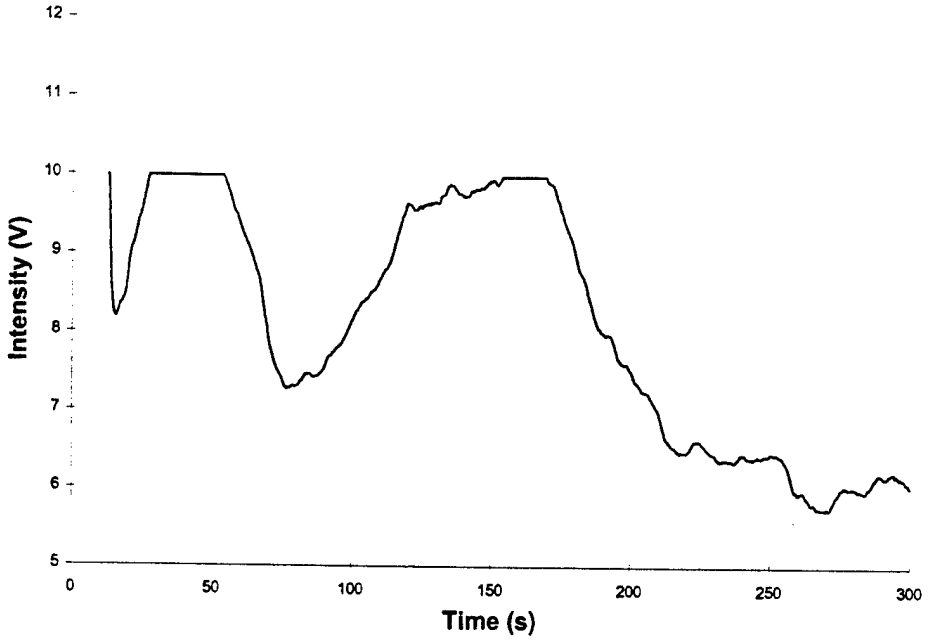

Fig.35 The variation of the photodetector signal as the interference pattern moves across the slit as the sample is loaded. Each of the first two dips represents a dark fringe.

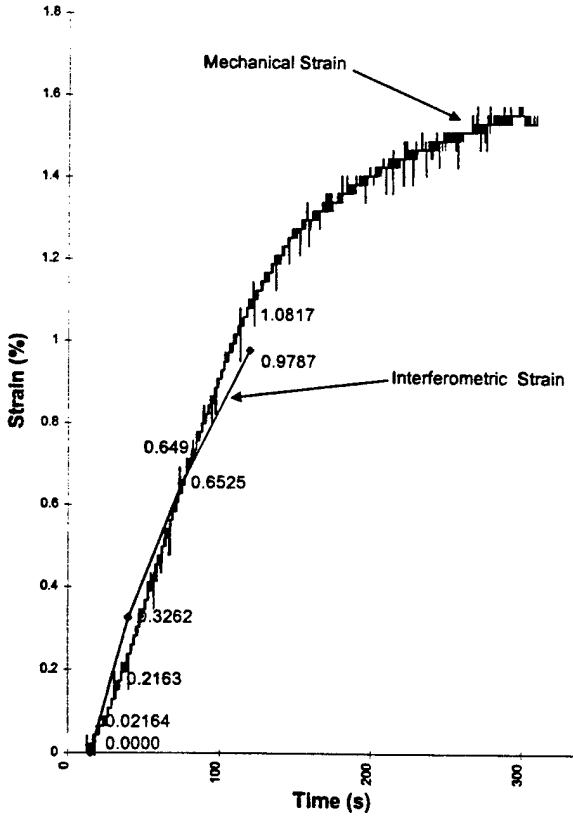

Fig.36 Comparison of the standard MTS results with that of the IDSG for 3 Point Bending measurements on an aluminum sample.

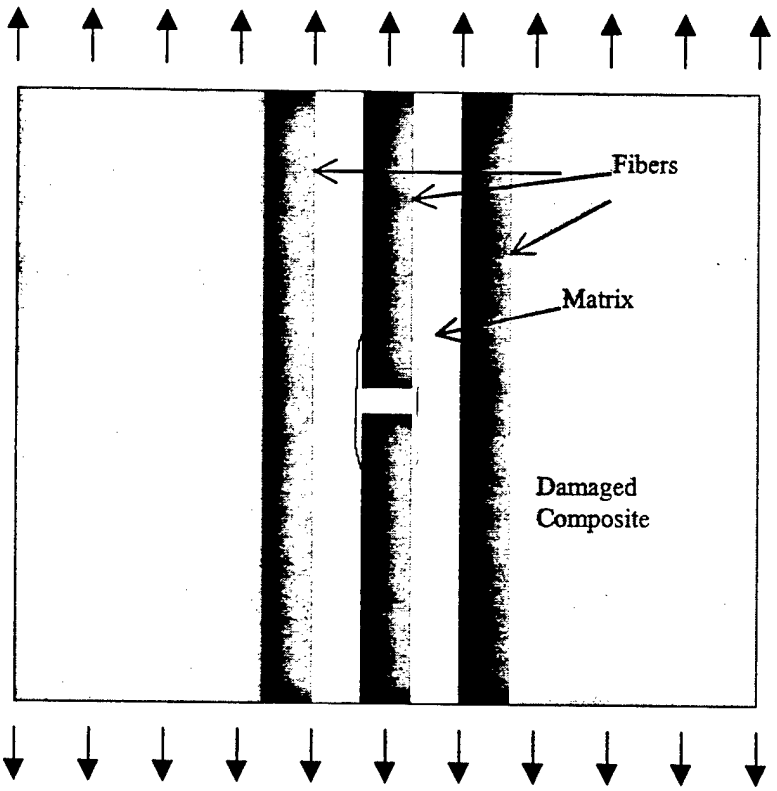

Fig.37 Three-Fiber Model of Unidirectional Lamina Damaged by Fiber Break.

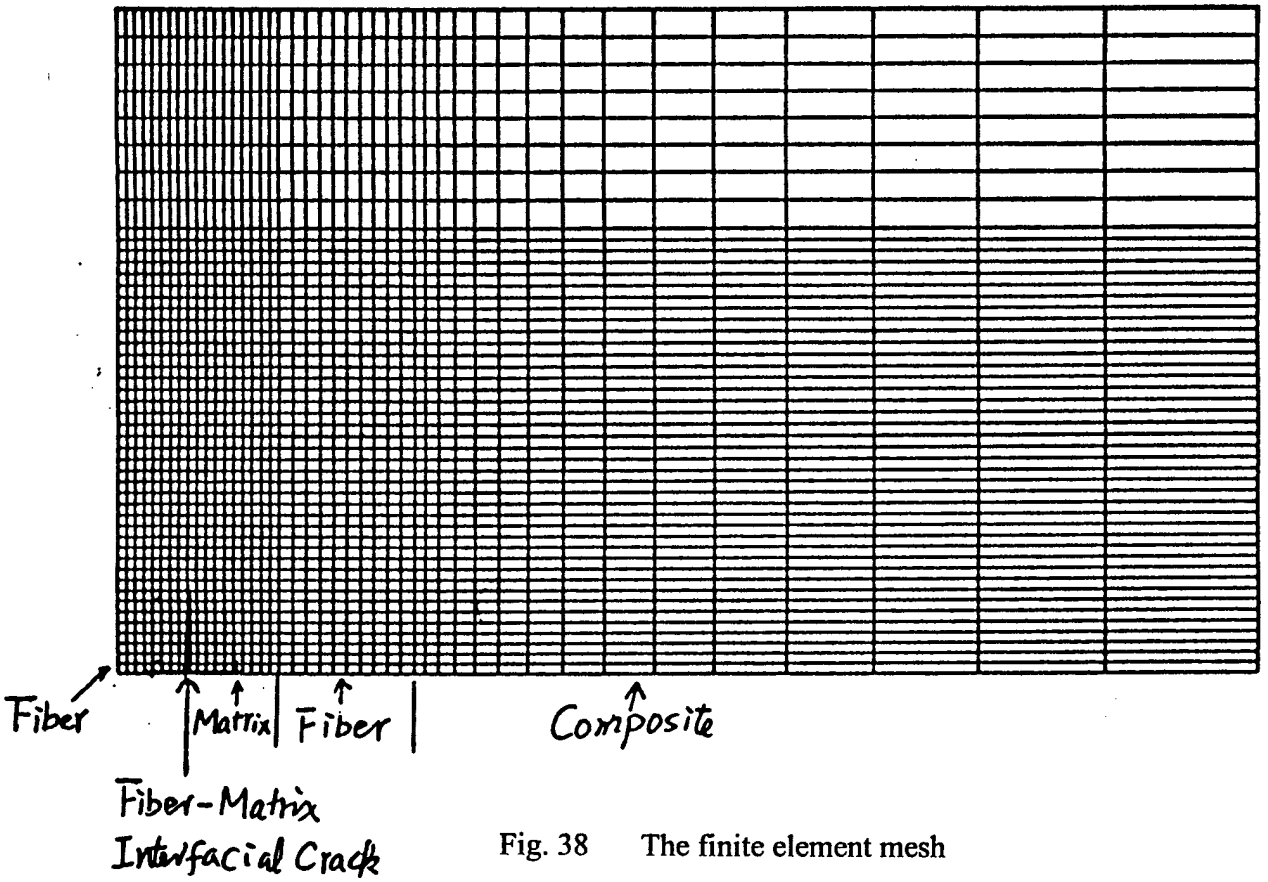

Fig. 38 The finite element mesh

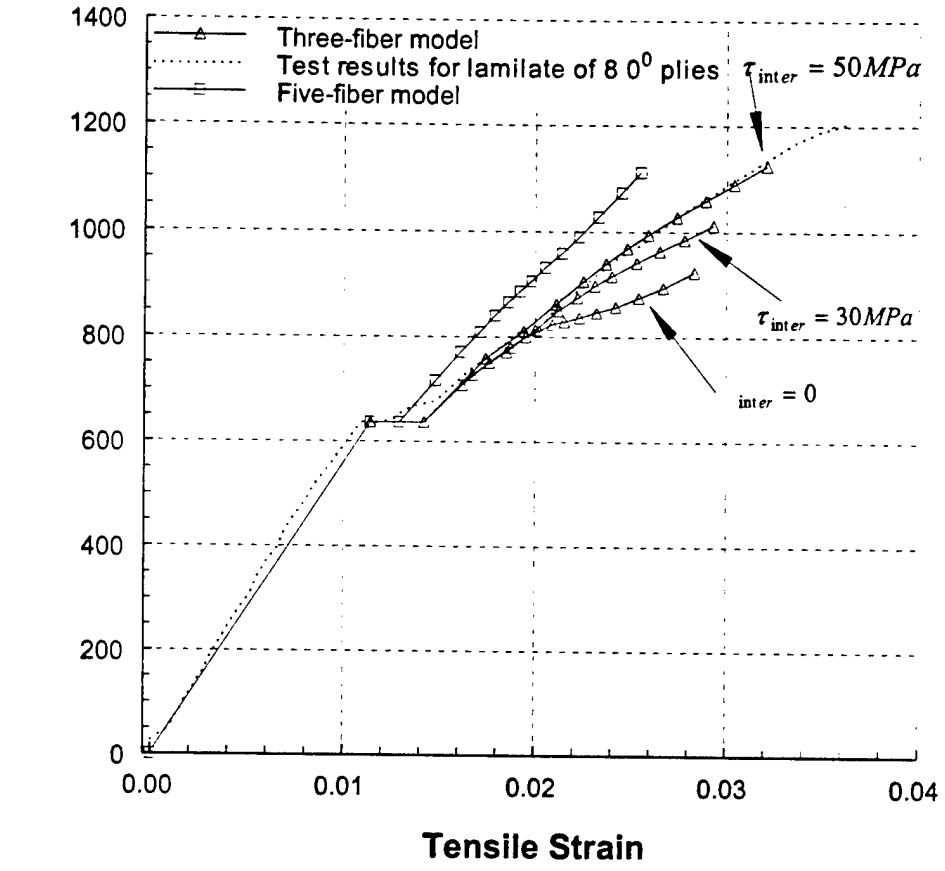

Fig.39 Comparison between simulated FE and experimental stress-strain curves for S2 glass toughened epoxy $[0^0]_{8\text{-ply}}$

Table 1. Lay-up configurations for specimens used in MTS tensile testing

Matrix: Newport NCT-301 Toughened Epoxy

Fibers: Owens Corning S2 Glass
Tape Code: 91C, 20 End Glass, OCF S-2 449AA 750 yd/lb

Fiber Vloume Fraction: 55%

Lay-Up Configurations:

Item	Qty	Dimensions	Thickness	Lay-up Configuration
1	40	Tpye 1	12-ply	$[0^0]_{12\text{-ply}}$
2	40	Tpye 2	12-ply	$[0^0]_{12\text{-ply}}$
3	40	Tpye 2	24-ply	$[0^0]_{24\text{-ply}}$
4	40	Tpye 1	24-ply	$[90^0]_{24\text{-ply}}$
5	40	Tpye 1	12-ply	$[0^0/90^0/0^0/90^0/0^0/90^0]_{symmetric}$
6	40	Tpye 1	24-ply	$[0^0/0^0/90^0/90^0/0^0/0^0/90^0/90^0/0^0/0^0/90^0/90^0]_{symmetric}$
7	40	Tpye 1	24-ply	$[90^0/90^0/0^0/0^0/90^0/90^0/0^0/0^0/90^0/90^0/0^0/0^0]_{symmetric}$
8	40	Tpye 1	12-ply	$[+45^0/-45^0/+45^0/-45^0/+45^0/-45^0]_{symmetric}$
9	40	Tpye 1	24-ply	$[+45^0/+45^0/-45^0/-45^0/+45^0/+45^0/-45^0/-45^0/+45^0/+45^0/-45^0/-45^0]_{symmetric}$
10	40	Tpye 1	24-ply	$[0^0/0^0/0^0/+45^0/+45^0/+45^0/90^0/90^0/90^0/-45^0/-45^0/-45^0]_{symmetric}$
11	40	Tpye 1	24-ply	$[90^0/90^0/90^0/+45^0/+45^0/+45^0/0^0/0^0/0^0/-45^0/-45^0/-45^0]_{symmetric}$
12	40	Tpye 1	24-ply	$[+45^0/+45^0/+45^0/0^0/0^0/0^0/-45^0/-45^0/-45^0/90^0/90^0/90^0]_{symmetric}$

Table 2. Lay-up configurations for specimens used in MTS 3-point bending testing

Matrix: Newport NCT-301 Toughened Epoxy

Fibers: Owens Corning S2 Glass
Tape Code: 91C, 20 End Glass, OCF S-2 449AA 750 yd/lb

Fiber Vloume Fraction: 55%

Lay-Up Configurations:

Item	Qty	Dimensions	Thickness	Lay-up Configuration
1	40	Tpye 1	24-ply	$[0^0]_{12\text{-ply}}$
2	40	Tpye 1	24-ply	$[90^0]_{24\text{-ply}}$
3	40	Tpye 1	24-ply	$[0^0/0^0/0^0/90^0/90^0/90^0/0^0/0^0/0^0/90^0/90^0/90^0]_{symmetric}$
4	40	Tpye 1	24-ply	$[90^0/90^0/90^0/0^0/0^0/0^0/90^0/90^0/90^0/0^0/0^0/0^0]_{symmetric}$
5	40	Tpye 1	24-ply	$[+45^0/+45^0/+45^0/-45^0/-45^0/-45^0/+45^0/+45^0/+45^0/-45^0/-45^0/-45^0]_{symmetric}$
6	40	Tpye 1	24-ply	$[0^0/0^0/0^0/+45^0/+45^0/+45^0/90^0/90^0/90^0/-45^0/-45^0/-45^0]_{symmetric}$
7	40	Tpye 1	24-ply	$[90^0/90^0/90^0/+45^0/+45^0/+45^0/0^0/0^0/0^0/-45^0/-45^0/-45^0]_{symmetric}$
8	40	Tpye 1	24-ply	$[+45^0/+45^0/+45^0/0^0/0^0/0^0/-45^0/-45^0/-45^0/90^0/90^0/90^0]_{symmetric}$
9	30	Tpye 2	24-ply	$[0^0]_{24\text{-ply}}$
10	30	Tpye 2	24-ply	$[0^0/0^0/0^0/90^0/90^0/90^0/0^0/0^0/0^0/90^0/90^0/90^0]_{symmetric}$
11	30	Tpye 2	24-ply	$[+45^0/+45^0/+45^0/-45^0/-45^0/-45^0/+45^0/+45^0/+45^0/-45^0/-45^0/-45^0]_{symmetric}$
12	30	Tpye 2	24-ply	$[0^0/0^0/0^0/+45^0/+45^0/+45^0/90^0/90^0/90^0/-45^0/-45^0/-45^0]_{symmetric}$

Table 3. Comparison of theoretical and experimental values of stiffness for various lay-up configurations

Configuration	E_c (GPa) Experimental	E_c (GPa) Theoretical	Error %
$[0^0]_{8\text{-ply}}$	50	51.9	1.90
$[0^0/90^0/0^0/90^0]_{symmetric}$	25	35.1	10.10
$[0^0/+45^0/90^0/-45^0]_{symmetric}$	17.5	27.3	9.80
$[+45^0/-45^0/+45^0/-45^0]_{symmetric}$	14	19.5	5.50

Table 4. Variation of stiffness and strength of the composite with various lay-up configurations

Configuration	Stiffness [MPa]	Strength [MPa]
$[0^0]_{24\text{-ply}}$	45000	950
$[0^0/0^0/90^0/90^0/0^0/0^0/90^0/90^0/0^0/0^0/90^0/90^0]_{symmetric}$	25500	600
$[0^0/0^0/0^0/+45^0/+45^0/+45^0/90^0/90^0/90^0/-45^0/-45^0/-45^0]_{symmetric}$	21000	310
$[+45^0/+45^0/-45^0/-45^0/+45^0/+45^0/-45^0/-45^0/+45^0/+45^0/-45^0/-45^0]_{symmetric}$	14000	120

APPENDIX A

Description of Phase II of Project

TESTING AND ANALYSIS OF COMPOSITE JOINTS AT ROOM AND ELEVATED TEMPERATURES

By

F. Delale, A. Walser, B M. Liaw

A PREPROPOSAL SUBMITTED TO U.S. ARMY TANK-AUTOMOTIVE COMMAND

JUNE 1997

INTRODUCTION

Our current research under contract with U.S. Army Tank-Automotive Command (TACOM) is on testing and analysis of composites for damage evaluation at room and elevated temperatures. The composite being tested is Newport NCT-301/S2, a toughened epoxy matrix/ S-glass fiber thermoset composite manufactured by Composiflex, Inc. Composite specimens of various lay-up configurations are being tested first in situ in a scanning electron microscope (SEM) and then using a universal testing machine both at room and elevated temperatures . The damage in the com posite is recorded through microphotographs and expressed quantitatively through a stress-strain curve constructed from the experimental data. After on-set of damage this curve becomes in general non-linear depending on the type and severity of the damage. To simulate this behavior a finite element model based on micromechanics and taking into consideration the actual damage observed has been developed. This research is expected to be completed before the end of 1997.

As continuation of this research we would like to extend this study to the testing and analysis of composite joints as contemplated in our original proposal. We realize that the topic of composite joining is technologically one the most challenging areas of composites research that can easily overwhelm the best equipped laboratory. For this reason in our preproposal we will list several possible venues of research within the technological capability of our laboratory and hope that with the feedback we will receive from the TACOM research personnel we can develop a research program which may be of use to the U.S. Army.

The joining of composites presents such technological and design problems that any design engineer ,if possible, would avoid it. The reasons for this are well known: stress concentration around holes; damage of fibers during drilling of holes; exposure of fibers to environmental agents; and in case of adhesive bonding : stress concentration at the edges, surface preparation of adherends, compatibility of adhesive and adherends, large deformations under fatigue loads, etc. But since it is not possible to completely avoid joints, it is necessary to understand the problems associated with them. In joining composites there are basically three practical technologies: joining with mechanical fasteners, adhesive bonding, and use

of mechanical fasteners in combination with adhesive bonding. (There are newer technologies for thermoplastic composites such as ultrasonic and laser welding, induction bonding, dual resin bonding, resistance heating, focused infrared energy, etc. But these are mostly still in the development stage.)

As mechanical fasteners one may use rivets or bolts. Mechanical fasteners may be aluminum, stainless steel, titanium alloys (because of cost they are used mainly in aerospace applications), or even composite (such as the Composi-Lok blind bolt, the Live Lock fastener, or the Comp-Tite fastener used in composite to composite applications.). Use of mechanical fasteners usually requires the drilling of holes which may cause many problems. As pointed out earlier in this case the problems to consider are : stress concentration around holes, fiber damage during drilling, exposure of fibers to environmental agents causing moisture absorption and delamination, thermal stresses due to different thermal expansion coefficients of composite and fastener. In case of direct contact with graphite fibers fasteners may be corroded. This may then require coating of the hole surface, thus creating more problems.

In adhesively bonded joints many of the problems mentioned above are avoided. However, adhesive bonding is not without problems. The problems associated with adhesive bonding are : stress concentration at the edges, compatibility of adhesive and adherends, surface preparation of adherends, large deformation during fatigue loading. For thermoset composite adhesives that cure at room temperature are preferred. In high temperature applications the adhesive must also be high temperature resistant.

Adhesively bonded and bolted joints are best, because one may avoid the weaknesses of both, (such as shear out in bolted joints and interfacial shear in adhesive bonds) , but obviously are more expensive to manufacture.

In studying joints there are many configurations to consider: lap joints (single-lap joint, double-lap joint, stepped-lap joint), strap joints (single-strap joint, double-strap joint, tapered-strap joint), and scarf joints. There are advantages and disadvantages associated with each configuration.

PROPOSED RESEARCH

As continuation of our current research we propose to test and analyze composite joints made of NCT-301/S2 plies. The parts to be joined will be 24 plies each and will be configured as double-strap joints. The joining will be through stainless steel bolts. A schematic rendering

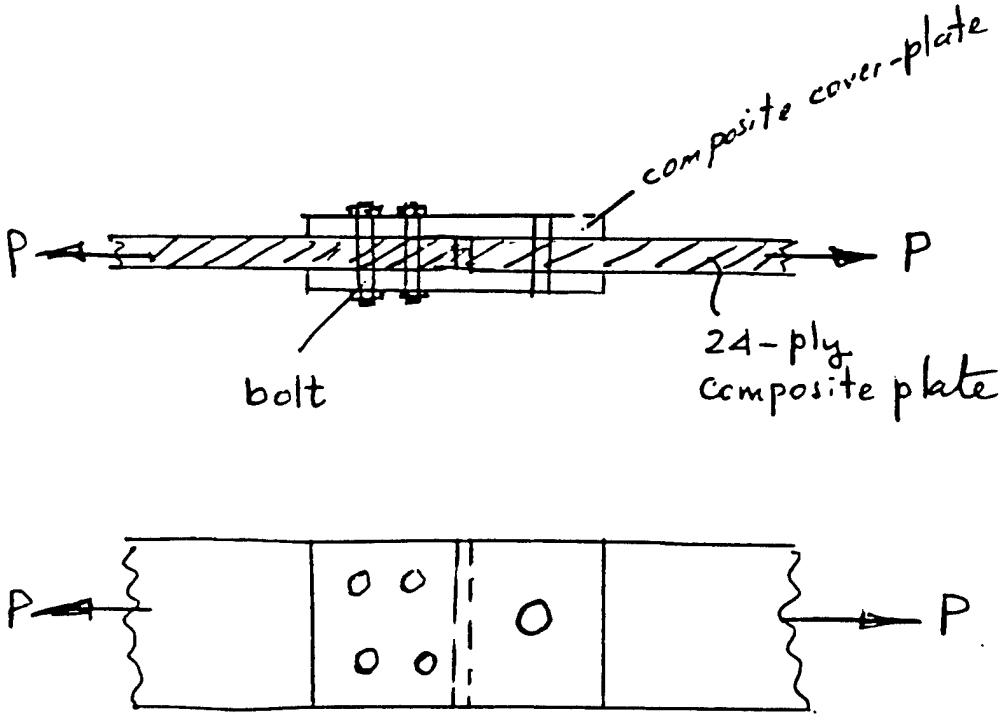

Fig 1.

of the joint is shown in Figure 1.

The reason for choosing this configuration is ease of testing due to its symmetry and gripping conditions. Several lay-up configurations will be tested : $[0^{\circ}]_{24\text{-ply}}$; $[90^{\circ}]_{24\text{-ply}}$; $[0^{\circ}/0^{\circ}/90^{\circ}/90^{\circ}/0^{\circ}/0^{\circ}/90^{\circ}/90^{\circ}/0^{\circ}/0^{\circ}/90^{\circ}/90^{\circ}]_S$; $[90^{\circ}/90^{\circ}/0^{\circ}/0^{\circ}/90^{\circ}/90^{\circ}/0^{\circ}/0^{\circ}/90^{\circ}/90^{\circ}/0^{\circ}/0^{\circ}]_S$; $[+45^{\circ}/+45^{\circ}/-45^{\circ}/-45^{\circ}/+45^{\circ}/+45^{\circ}/-45^{\circ}/-45^{\circ}/+45^{\circ}/+45^{\circ}/-45^{\circ}/-45^{\circ}]_S$; $[0^{\circ}/0^{\circ}/0^{\circ}/+45^{\circ}/+45^{\circ}/+45^{\circ}/90^{\circ}/90^{\circ}/90^{\circ}/-45^{\circ}/-45^{\circ}/-45^{\circ}]_S$; $[90^{\circ}/90^{\circ}/90^{\circ}/+45^{\circ}/+45^{\circ}/+45^{\circ}/0^{\circ}/0^{\circ}/0^{\circ}/-45^{\circ}/-45^{\circ}/-45^{\circ}]_S$; and $[+45^{\circ}/+45^{\circ}/+45^{\circ}/0^{\circ}/0^{\circ}/0^{\circ}/-45^{\circ}/-45^{\circ}/-45^{\circ}/90^{\circ}/90^{\circ}/90^{\circ}]_S$. As stated earlier this is a thermoset epoxy / S2 glass composite and we are quite familiar with its properties. The joints will be tested in the MTS machine until failure. The failure load , failure modes and strains at various locations of the joint will be recorded. The joints will be tested at room , 75° C , and 125° C . For the latter tests an environmental chamber will be used. The holes in the composite may be left in their natural state or coated with epoxy to insulate them from environmental damage. Also the cover plates in the strapped joints may be glued with epoxy to the composite plates in addition to bolts or only bolts may be used.

The stresses and strains in the composite plates will be analyzed using a finite element model. The following issues will be considered : stress concentration around holes, bearing stresses (contact stresses between bolt and composite) , shear-out stresses in the composite plates, initiation and propagation of delamination from hole boundary. In case of high temperature thermal stresses due to thermal expansion mismatch will be considered. It is believed that a model explaining the observed damage sequence can be developed.

The above description outlines our ideas for research on composite joints. We would like to get feedback from Army personnel so that this program can be relevant and complimentary to research and development efforts at TARDEC.

APPENDIX B

Abstracts Submitted for Presentation

DAMAGE BEHAVIOR OF S2 GLASS/ TOUGHENED EPOXY COMPOSITES UNDER TENSILE LOADING

by

F. Delale, B.M. Liaw, C.K. Cheung, A.D. Walser

The City College of CUNY

and

B.B. Raju

U.S. Army Tank-Automotive Research, Development & Engineering Center

EXTENDED ABSTRACT

In this study the damage behavior of S2 Glass/Toughened Epoxy Composites was investigated under tensile loading and room temperature conditions. The composite was manufactured and made into 8-ply 2.5"x4" panels of various configurations by Composiflex, Inc. with fiber volume fraction of 55%. The following lay-up configurations were used : $[0^\circ]_8$, $[0^\circ/90^\circ]_{2s}$, $[0^\circ/+45^\circ/90^\circ/-45^\circ]_{2s}$ and $[\pm 45^\circ]_{2s}$. First, miniature dog-bone shaped specimens for a Scanning Electron Microscope (SEM) were machined at CCNY in the Materials Processing Laboratory. The surfaces of the specimens were polished for SEM observations, then the specimens were mounted onto a loading/heating substage and put in the chamber of SEM. The load was increased until failure and the corresponding displacements were recorded. The progression of damage was monitored on the screen of the SEM and when warranted microphotographs were taken. The load and displacement data were converted to stresses and strains respectively and a tensile stress-strain curve was constructed.

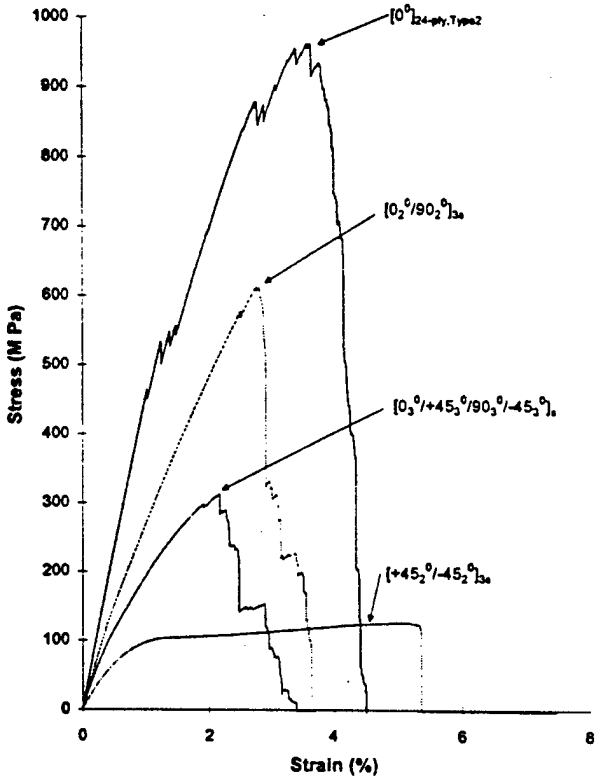

Fig 1. Composite Material (S2 glass toughened epoxy) at Room Temperature

The stress-strain curves as expected are first linear and later become non-linear due to fiber

*This study was supported by U.S. Army TACOM/TARDEC under contract DAAE07-96-C-X121

All correspondence should be directed to:
Prof. F. Delale, Dept. of Mechanical Engineering, The City College Of CUNY
138th & Convent Ave., New York, N.Y. 10031
Tel: (212) 650-5224; Fax: (212) 650-8013; E-mail: delale@med3cd.engr.ccny.cuny.edu

breaking and interfacial debonding. It was observed that the ultimate failure strength varied considerably with the lay-up configuration, obviously the highest strength obtained with the $[0^0]_8$ specimens.

Next dog-bone shaped larger size specimens of the same composite were tested in an Universal Testing Machine (MTS), for the following configurations: $[0^0]_{24\text{-ply}}$, $[0_2{}^0/90_2{}^0]_{3s}$, $[0_3{}^0/+45_3{}^0/90_3{}^0/-45_3{}^0]_s$ and $[+45_2{}^0/-45_2{}^0]_{3s}$. For each lay-up at least 4 specimens were tested. The results look quite consistent, without significant scattering. For all configurations the stress-strain curve has a linear portion corresponding to the undamaged state, followed by a non-linear portion corresponding to the damaged state. The shape of the non-linear portion varies with the various lay-up configurations, which have different failure modes. The effect of lay-up can be clearly seen in Fig. 1, where the results for the four configurations are plotted together. It is observed that the failure strength, stiffness and failure strain of the composite are highly affected by the lay-up architecture.

An analytical model to simulate the observed behavior and based on micromechanics was developed. It was observed that the model based on finite element calculations and incorporating the elastic properties of matrix and fiber, and interfacial shear can simulate the observed behavior quite well (Fig.2.)

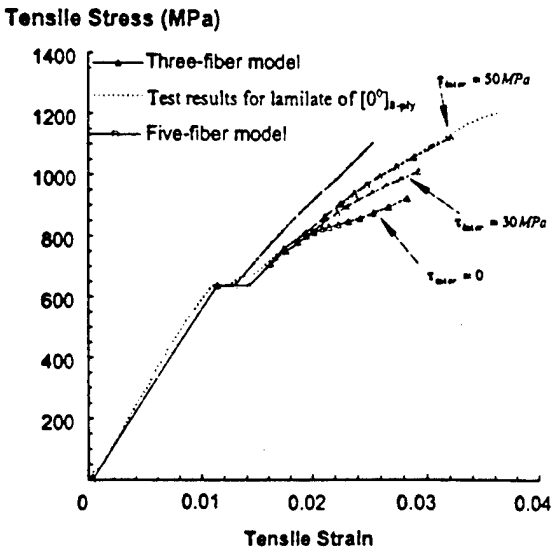

Fig. 2. Comparison between simulated FE and experimental stress-strain curves for S2 glass toughened epoxy ($[0^0]_{8\text{-ply}}$)

Abstract for the 13th Annual Technical Conference, American Society for Composites
Sheraton Hotel, Inner Harbor, Baltimore, Maryland, September 21-23, 1998

BENDING-INDUCED DAMAGES IN S2 GLASS/TOUGHENED EPOXY COMPOSITES AT ROOM AND ELEVATED TEMPERATURES*

by

C. K. Cheung, B. M. Liaw, F. Delale, A. D. Walser
The City College of CUNY

and

B. B. Raju
U. S. Army Tank-Automotive Research Development & Engineering Center

ABSTRACT

Three-point bending tests of S2 glass/toughened epoxy composites of various lay-up configurations were conducted at room and elevated temperatures (75 and 125°C). The lay-up configurations of these 24-ply toughened thermoset composites were: $[0]_{24}$, $[0_2/90_2]_{3S}$, $[\pm45_2]_{3S}$ and $[0_3/45_3/90_3/-45_3]_S$. Specimens of two sizes (10″×1″×¼″ and 10″×¼″×¼″) subject to three-point loading were tested in an MTS universal testing machine equipped with an environmental chamber and the mid-point deflection was recorded. Unlike stress-strain curves of the same material under tension loading, which resembled those of quasi-brittle materials for $[0]_{24}$ and $[0_2/90_2]_{3S}$ configurations and of quasi-ductile materials for the $[\pm45_2]_{3S}$ configuration, loading-deflection curves resulting from 3-point bending tests were more varied after the occurrence of initial failure. This difference can be explained from photographic evidence taken during tests. In direct tension tests, matrix cracking and fiber breaking were the main cause for the quasi-brittle like behavior of $[0]_{24}$ and $[0_2/90_2]_{3S}$ specimens whereas failure due to in-plane shear resulted in the quasi-ductile response of $[\pm45_2]_{3S}$ specimens. In 3-point bending tests, mixed-mode failure was predominant. In particular, delamination (which rarely took place in tension tests) occurred frequently in bending tests. The phenomenon, of course, can be attributed to the nonuniform stress distribution across layers. Our results also show that though not as important as in tension tests, temperature also had some effect. In a nut shell, higher temperature reduce the maximum load that a specimen could take; thus lowering the specimen's modulus of rupture. Other than that, the loading-deflection curves of specimens with the same configuration at various temperatures were similar.

---

* This investigation was supported by U. S. Army TACOM/TARDEC under Contract DAAE07-96-C-X121.

Future correspondence should be directed to:

Professor Benjamin Liaw
City College of New York
Department of Mechanical Engineering
Convent Avenue & 138th Street
New York, NY 10031

Tel: (212) 650-5204
Fax: (212) 650-8013
E-mail: liaw@me-mail.engr.ccny.cuny.edu

Abstract for the 13th Annual Advanced Composite Conference - ACCE'98
Cobo Center, Detroit, Michigan, September 28-29, 1998

TENSION-INDUCED DAMAGES OF S2 GLASS/TOUGHENED EPOXY COMPOSITES AT ROOM AND ELEVATED TEMPERATURES*

by

B. M. Liaw, C. K. Cheung, F. Delale, A. D. Walser
The City College of CUNY

and

B. B. Raju
U. S. Army Tank-Automotive Research Development & Engineering Center

ABSTRACT

Tensile tests of S2 glass/toughened epoxy composites of various lay-up configurations were conducted at room and elevated temperatures. The lay-up configurations of these 24-ply toughened thermoset composites were: $[0]_{24}$, $[0_2/90_2]_{3S}$, $[\pm 45_2]_{3S}$ and $[0_3/45_3/90_3/-45_3]_S$. Miniature dog-bone shaped specimens were first tested *in situ* in a scanning electron microscope (SEM) under tensile loading and at three temperature conditions: room temperature, 75°C and 125°C. Progression of damage patterns was photographed and the corresponding stresses and strains were recorded from the first crack to complete failure of specimens. Standard-size specimens of the same material were then tested in an MTS universal testing machine equipped with an environmental chamber. It was found that the non-linear stress-strain curves obtained from these two testing schemes were compatible. Depending on lay-up configuration, the stress-strain relations looked like curves for quasi-brittle materials for the $[0]_{24}$ and $[0_2/90_2]_{3S}$ specimens whereas for the $[\pm 45_2]_{3S}$ specimens, they resembled those of quasi-ductile materials. The mechanical behaviors of the $[0_3/45_3/90_3/-45_3]_S$ specimens, as expected, lay on the middle ground of the two extremes. Per evidence from SEM microfractographs, difference in damage-induced mechanical behaviors was attributed to their corresponding dominant failure modes. That is, matrix cracking, fiber-matrix debonding, and fiber pull-out and breaking characterized the quasi-brittle type of responses while shear failure and delamination were responsible for the quasi-ductile type of behaviors. In addition to lay-up configuration, temperature also played an important role. With the exception of the $[0_3/45_3/90_3/-45_3]_S$ configuration, ultimate tensile strengths of these composite specimens were reduced when tested at high temperature. For the $[0_3/45_3/90_3/-45_3]_S$ case, temperature effect was almost negligible. It is also interesting to note that the "ductilities" at break for the $[0]_{24}$ and $[0_2/90_2]_{3S}$ specimens were lowered at high temperature; whereas the "ductility" at break for the $[\pm 45_2]_{3S}$ specimens increased with temperature. Difference in this high-temperature characteristics can again be explained by their associated failure modes.

---

* This investigation was supported by U. S. Army TACOM/TARDEC under Contract DAAE07-96-C-X121.

Future correspondence should be directed to:

Professor Benjamin Liaw
City College of New York
Department of Mechanical Engineering
Convent Avenue & 138th Street
New York, NY 10031

Tel: (212) 650-5204
Fax: (212) 650-8013
E-mail: liaw@me-mail.engr.ccny.cuny.edu